

# The Specialist Committee on Energy Saving Methods

## Final Report and Recommendations to the 28 th ITTC

### 1 INTRODUCTION

#### 1.1 Membership and Meetings

The Specialist Committee on Energy Saving Methods (SC-ESM) was appointed by the 27th ITTC in Copenhagen, Denmark, 2014, and it consists of the following members (see picture in Figure 1):

- Mr. Tom Dinham-Peren, BMT (Chairman), BMT Defence Services Ltd, UK
- Professor Marc Perlin, University of Michigan, USA (Acting Chairman since Feb 2017)
- Dr. Joseph Banks, University of Southampton, UK. (Secretary)
- Professor Munehiko Hinatsu, Osaka University, Japan
- Mr. Michio Takai, Sumitomo Heavy Industries Marine & Engineering Co. Ltd., Japan
- Professor Decheng Wan, Shanghai Jiao Tong University, China
- Dr. Haeseong Ahn, Korea Research Institute Ships and Ocean Engineering, Korea
- Professor Inwon Lee, Pusan National University, Korea
- Dr. Mahdi Khorasanchi, University of Strathclyde, UK

Five Committee meetings were held as follows:

- BMT Defence Services Ltd, UK, 12 – 13 February 2015
- Osaka University, Japan, 30–31 November

2015

- Shanghai Jiao Tong University, China, 16–17 May 2016
- Texas A & M University, USA, 15–16 February, 2017
- University of Southampton, UK, 18 – 19 May 2017.

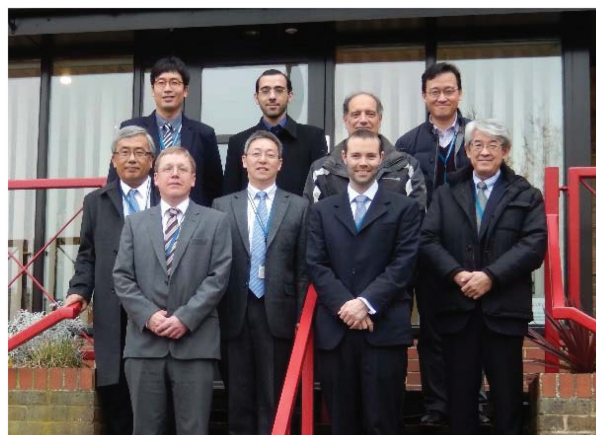


Figure 1 Photograph of ESM attendees at BMT Defence Services.

#### 1.2 Terms of Reference of the 27th ITTC

In its Terms of Reference (ToR) document, the 27th ITTC mandated the SC-ESM to perform the following Tasks:

(1) Conduct a systematic survey of energy saving methods (excluding machinery), devices, applications and possible savings, including the influence on the EEDI formula.

(2) Identify the physical mechanisms on energy saving on ships.

(3) Conduct a survey on frictional drag reduction methods, including air lubrication and surface treatment.

(4) Conduct a survey on energy savings based on the use of wind energy.

(5) Monitor the CFD methods, model tests and scaling procedures for energy saving devices.

(6) Conduct a survey on existing full scale data on the effect of energy saving methods.

(7) Identify the needs for new model test procedures (resistance and propulsion, extrapolation methods) to investigate the effect of energy saving methods.

### 1.3 Liaison with Other Committees and Overlap on TORs

We have been in contact with the Performance of Ships in Service (PSS), Propulsion (PC) and Resistance Committees (RC), both by email and by joint meetings as follows;

- Joint meeting with RC and PSS, Osaka University, Japan, 1 December 2015.
- Joint meeting with PC and PSS, Shanghai Jiao Tong University, China, 18 May 2016.
- Workshop on New Progress of Energy Saving Methods, Shanghai Jiao Tong University, China, 19 May 2016.

This was to clarify areas of overlap, decide who will move such areas forward and to discuss areas of common interest.

### 1.4 General Comments

As the first item of our ToR implies, there will be a multitude of approaches to save energy for marine vessels. Although there has been recent progress in retrofit devices to enhance propulsion efficiency, which are commonly described as “energy saving devices”, it is also important to remember that the potential scope of energy saving methods are quite extensive including aspects of initial design and ship operation.

Good initial design for hull form and propeller with less power demand should always be addressed as a relevant energy saving meth-

od. Historically, much effort has been made to reduce wavemaking resistance by bulbous bow and bow hull optimization. It must be emphasized that design is aimed at good performance not only for the model test/trial condition in ‘calm seas’ but also for the service conditions with wind and waves. Optimised hull forms to minimise added resistance in waves is a good example of a design approach to energy saving.

Many energy saving methods can be characterised as suitable for retrofit with the aim of reducing drag or the propulsive losses for an existing design. In addition these measures are often applicable to the initial design phase. Examples would include air lubrication and low frictional coatings for reducing resistance. On the other hand, there are devices designed to control the flow around the propeller to reduce propulsive losses. Use of renewable energy, such as wind and solar, also falls in this category.

The final category would deal with the optimal operation. Being free from additional investment, this is often regarded as the most effective approach by ship operators. Examples of this category include slow steaming, hull/propeller cleaning, weather routing and trim optimization, etc.

## 2 MECHANISMS AND UNDERLYING PHYSICS

The aim of an energy saving method is to reduce the power requirement of a ship without adversely affecting the vessel’s capability. To help understand where possible energy savings can be made, it is helpful to identify the physical mechanisms that contribute to the energy consumption of a ship.

Figure 2 provides a useful example of how the total propulsion energy for a small cargo ship is expended. This clearly demonstrates that a significant amount of energy is lost before it is delivered to the propeller shaft. How-

ever this report will focus on the mechanisms associated with ship resistance and propulsion

and will not cover aspects such as machinery efficiency and types of fuel etc.

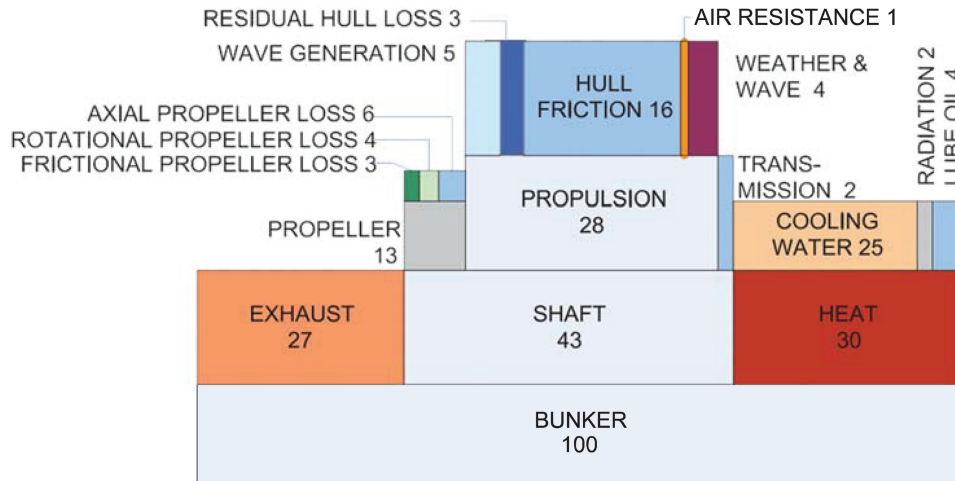


Figure 2 Energy breakdown of propulsion energy on board a small cargo ship in head seas, Beaufort 6 [International Maritime Organization, 2009]

The delivered power ( $P_D$ ) required by the propeller to achieve a constant speed is given by the equation:

$$P_D = \frac{R_T V_s}{\eta_D}$$

where  $R_T$  is the total resistance of the ship,  $V_s$  is the vessel speed and  $\eta_D$  is the Quasi Propulsive Coefficient (QPC), which represents the efficiency of the propeller whilst operating behind the ship.

Therefore, there are three main strategies for saving energy. Firstly, the vessel's speed can be reduced, however this will affect the operation of the ship. The second option is to reduce the total resistance of the vessel while operating at the same speed. The third option is to increase the ability of the propulsor to generate thrust whilst operating behind the vessel, thus increasing  $\eta_D$ .

## 2.1 Resistance Components

The total resistance acting on a vessel can

be split into different components depending on whether you are considering the forces acting on the hull or the dissipation of energy, as demonstrated in Figure.

The frictional resistance is due to the tangential/shear force exerted by the fluid on the hull. The no slip condition requires that the fluid immediately in contact with the hull has the same velocity as the hull's surface. Therefore a boundary layer forms whereby the fluid velocity varies from the vessel speed to the undisturbed fluid velocity. The energy lost to frictional resistance depends of the speed of the vessel, the wetted surface area and the surface properties. This will be discussed in more detail in section 3.

The pressure resistance is due to the local pressure distribution acting perpendicular to the hull surface, which when integrated generates a net force. The local pressure distribution is created by a mixture of viscous effects and the generation of waves on the free surface.

The wave making resistance defines the energy required to generate the wave pattern

behind the ship. It is dependent on the length and speed of the ship (i.e. the Froude number) and the hull form shape. The wave patterns generated by different parts of the hull can constructively or destructively interfere with each

other to increase or decrease the total energy in the wave pattern. Therefore the hull form can be modified to take advantage of this to minimise the wave resistance at a given ship speed.

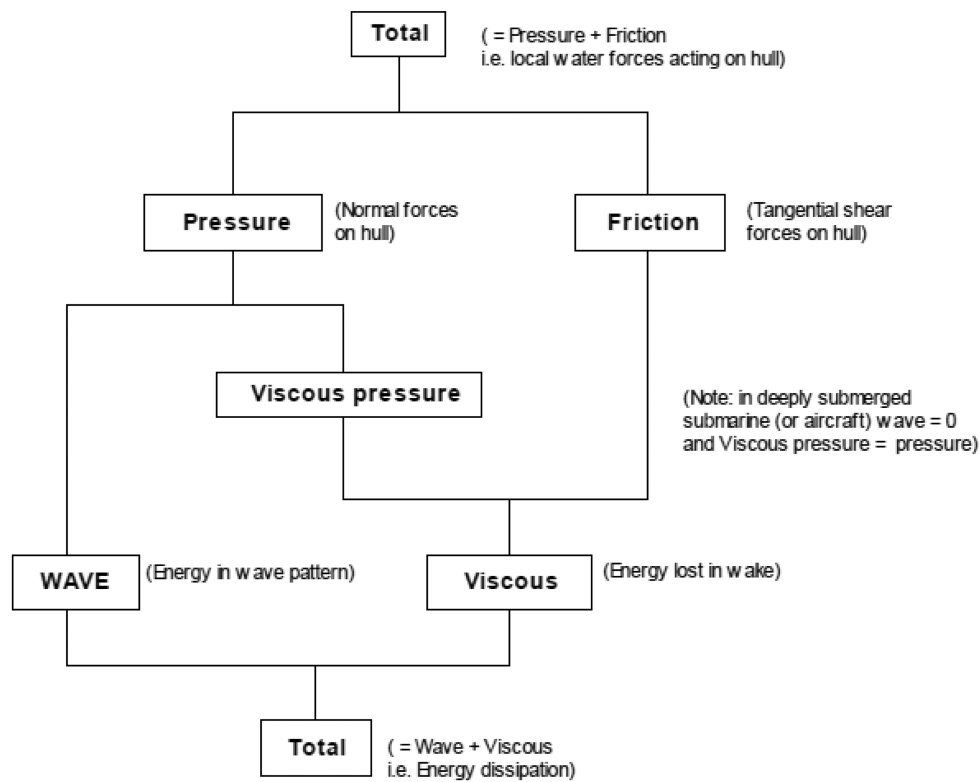


Figure 3 Breakdown of hull resistance components [Molland et al., 2014]

If the wave resistance is subtracted from the pressure resistance we are left with the viscous pressure drag (also known as the form drag). The viscous pressure resistance is associated with the pressure variations created by the viscous boundary layer and flow separation increasing the energy in the viscous wake. Flow separation occurs when areas of high curvature create an adverse pressure gradient causing the boundary layer to separate from the surface of the hull. This typically occurs around the stern sections of ships.

Figure 3 provides a breakdown of the total resistance for tankers and containerships. This clearly shows that the biggest component for these vessel types is the viscous resistance.

Table 1 provides a resistance breakdown for a wider range of vessels and splits the viscous resistance into friction and form drag. It can be observed that skin friction accounts for the majority of the total resistance (approximately 60%–70%) for most of the large commercial vessels. It is also apparent that as a vessel's speed increases, the proportion of wave resistance increases. This type of analysis helps identify the areas where improvement gains are likely to be made for different vessels.

It should be noted that the total resistance of a ship also includes the drag associated with appendages and the air resistance of the hull and superstructure. However these tend to be

smaller components (see Figure 4) and therefore offer reduced opportunities to make signif-

icant savings.

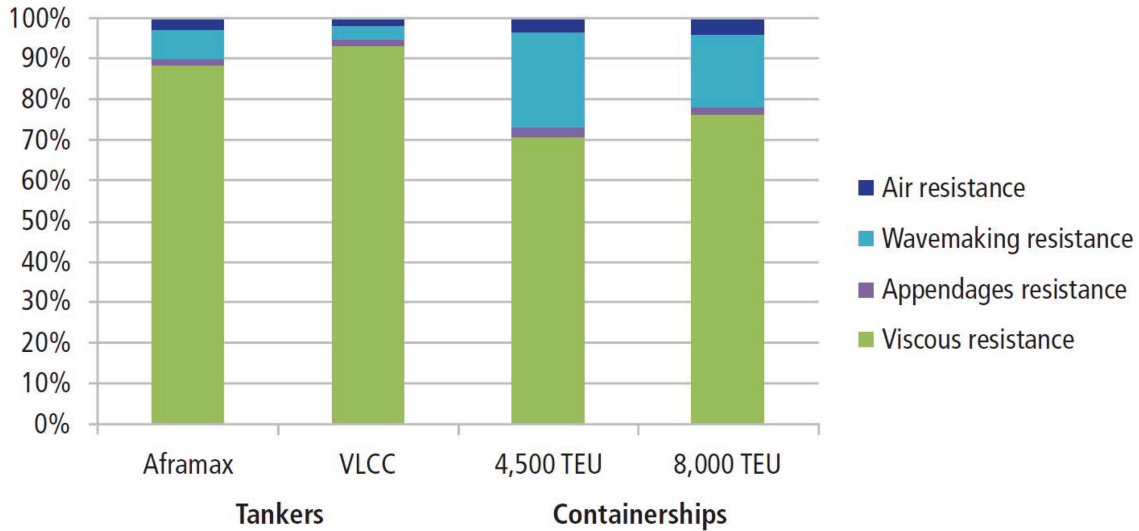


Figure 4 Components of calm water hull resistance at design speed [ABS guide]

Table 1 Approximate distribution of resistance components [Molland et al., 2014]

Type	L <sub>pp</sub> (m)	C <sub>B</sub>	D <sub>w</sub> (tonnes)	Service speed (Knots)	Service power (kW)	Fr	Hull resistance component			Air Drag % total
							Friction %	Form %	Wave %	
Tanker	330	0.84	250000	15	24000	0.136	66	26	8	2.0
Tanker	174	0.80	41000	14.5	7300	0.181	65	25	10	3.0
Bulk carrier	290	0.83	170000	15	15800	0.145	66	24	10	2.5
Bulk carrier	180	0.80	45000	14	7200	0.171	65	25	10	3.0
Container	334	0.64	100000 10000 TEU	26	62000	0.234	63	12	25	4.5
Container	232	0.65	37000 3500 TEU	23.5	29000	0.250	60	10	30	4.0
Catamaran ferry	80	0.47	650 pass 150 cars	36	23500	0.700	30	10	60	4.0

## 2.2 Propulsive Components

The effectiveness of a propeller to generate thrust whilst acting behind a ship is dependent on the propeller design and the flow field in which it operates due to the viscous wake of the ship. Froude initially combined self-propulsion tests with hull resistance and propeller open-water tests to help quantify and scale the propelled efficiency [Froude, 1883]. This ulti-

mately resulted in the quasi propulsive coefficient being defined as:

$$\eta_D = \eta_O \eta_H \eta_R$$

where

$\eta_O$  is the propeller open water efficiency,

$\eta_R$  is the relative rotative efficiency and

$\eta_H$  is the hull efficiency.



The propeller open water efficiency assesses the performance of the propeller in isolation, i.e. in an undisturbed flow.

The relative rotative efficiency accounts for the differences between a propeller operating in open water and behind a ship, such as in a non-uniform inflow and with higher levels of turbulence [Molland, 2011]. Typically values are between 0.98 and 1.02.

The hull efficiency takes into account the interaction between the hull and the propeller and can be calculated as:

$$\eta_H = \frac{(1-t)}{(1-w_T)}$$

where  $t$  is the thrust deduction factor and  $w_T$  is the wake fraction.

The thrust deduction accounts for the change in ship resistance due to the flow acceleration induced by the propeller. This increased flow velocity at the stern adds to the frictional resistance, and generally reduces the local pressure at the stern, increasing the form drag. It should also be noted that this change in the local pressure distribution can also affect flow separation compared to a naked hull.

As the propeller operates in the ship's viscous wake the average velocity of flow into the propeller ( $V_a$ ) is less than the ship's forward speed ( $V_s$ ) and is represented using the Taylor wake fraction:

$$w_T = \frac{(V_s - V_a)}{V_s}$$

Dyne [1994] split the open water propeller efficiency into different components based on different sources of energy loss. For a fixed set of propeller parameters (such as  $D$ ,  $P/D$  and rpm)

$$\eta_o = \eta_a \cdot \eta_r \cdot \eta_f$$

where  $\eta_a$  is the ideal (or axial) efficiency,  $\eta_r$  accounts for losses due to induced fluid rotation

and  $\eta_f$  accounts for losses due to blade friction drag.

Dyne [1995] observed that the propulsive efficiency  $\eta_D$  can be maximised by designing the propulsive system to recover as much of the energy in the ship's wake as possible.

Molland et al. [2014] investigated the relative proportions of the individual propeller efficiencies using blade element momentum theory. The investigated propeller had a pitch ratio  $P/D = 1.0$ ,  $BAR = 0.700$ , four blades, and was assessed for a range of  $J$  values.

It can be seen from Figure 5 that as the  $J$  value get larger (and the thrust loading  $C_T$  decreases) the frictional losses increase, while the rotation loss decreases and there is a significant reduction in the axial loss. For a design condition of  $J = 0.75$  ( $C_T = 0.86$ ), it can be seen that the losses are typically 60% axial, 10% rotational and 30% frictional.

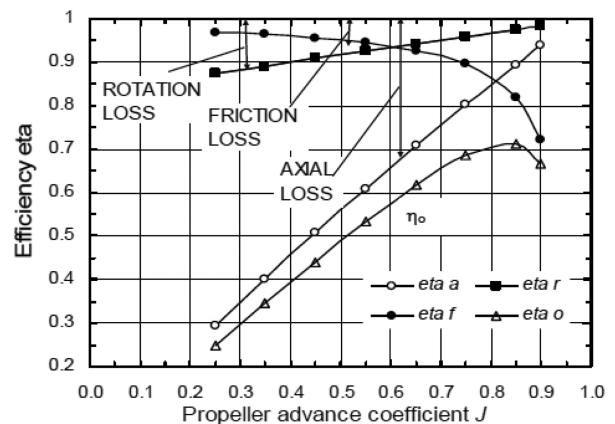


Figure 5 Components of propeller efficiency [Molland, 2014]

Axial or Ideal Efficiency  $\eta_a$ . The axial efficiency represents the kinetic energy of axial flow left in the wake behind the propeller. This is by far the largest propeller loss for most operating conditions and is strongly related to the propeller diameter. Increasing the propeller diameter while adjusting the  $P/D$  and rpm pro-

portionally, will reduce the axial induced velocity improving the axial efficiency [Molland 2014].

Rotative Efficiency  $\eta_r$ . This represents the swirl kinetic energy added to the wake behind the propeller. Various approaches are available to try to recover this energy including:

- Contra rotating propellers, which aim to remove the rotational energy;
- Pre or post swirl stators, which generate thrust from realigning the flow;
- Rudder design aimed at flow alignment.

These devices tend to increase the frictional resistance due to increased wetted surface area; therefore improvements in propulsive efficiency need to outweigh this to achieve an overall gain.

Friction Efficiency  $\eta_f$ . The energy loss due to propeller friction is related to the propeller surface area, surface finish and local flow velocity. The friction efficiency can be improved by reducing the inflow velocity with a reduction in revolutions and either increasing the propeller diameter or increasing the blade pitch [Molland 2014].

In reality to achieve the best propulsive efficiencies the interactions between the hull and the propulsor need to be fully considered. In an ideal scenario the axial kinetic energy added to the wake by the propulsor would exactly balance the axial wake behind the ship. Likewise any rotational energy within the wake of the hull would be recovered as part of the propulsion system.

### 2.3 Renewable Sources of Propulsion

A different way to improve the efficiency of a vessel is to augment the thrust from traditional propulsion sources with that obtained from renewable energy. This reduces the shaft power required to travel at the same speed. One obvious example of this covered in more detail

in section 4 is wind assisted ships.

### 2.4 Current Application and Effectiveness

A report on energy management in the shipping industry [DNVGL, 2015] included the responses of 80 shipping companies regarding energy saving measures they had already implemented. This highlighted that nine simple energy saving measures had already been implemented by over 50% of the companies. These measures were predominantly operational including hull/propeller cleaning, slow steaming and performance monitoring etc. When asked ‘What are the top three measures that contributed to fuel reduction in your fleet in 2014?’, slow steaming was ranked first followed by hull/propeller cleaning and voyage planning optimisation.

For a summary of the potential savings from different energy saving methods, refer to the different industry reports in this area [DNVGL, 2015; SOCP, 2016; OCIMF, 2011; ABS, 2015].

## 3 FRICTIONAL DRAG REDUCTION METHODS

In general, skin-friction drag reduction (FDR) is any of several available methods that alter the skin friction that would exist in the method’s absence. These approaches are discussed below in limited detail; however several texts cover the various methods, the most recent of which is the book by Perlin and Ceccio (2015) entitled Mitigation of Hydrodynamic Resistance. FDR methods include both passive and active techniques. Passive methods, which as the name implies are implemented with no further action required (until they perhaps degrade), include textured surfaces such as riblets, compliant surfaces, large-eddy breakup devices, super-hydrophobic surfaces, and surface coatings/paints. Active methods require energy and/or other input, and include such methods as

polymer injection, gas injection (bubbles, layers and cavities), heating/cooling and wall motion/deformation. A very recent review (Perlin, Dowling and Ceccio, 2016) discusses FDR in the context of general fluid mechanics rather than from the point of view of ships and objects moving in the oceans. Another recent text that includes discussions of more general friction drag reduction techniques for turbulent flows is that of Gyr and Bewersdorff (2013) entitled Drag Reduction of Turbulent Flows by Additives.

In the discussion that follows, review-manuscript references are provided where available for each of these techniques, and subsequently references and brief discussions of the most recent literature (approximately four years or so) are presented. Unless otherwise stated, herein when we present FDR results, these are with respect to the total friction rather than as a percent or fraction of the total drag.

### 3.1 Passive Methods

Riblets and other textured surfaces. Walsh (1983) and Choi (1989) discuss riblets that they define as texturing applied longitudinally on a surface, which are typically shaped as triangular waves, cusps, or rectangles, and have been shown to generate about 10% friction drag reduction. Unlike many of the other surfaces to be discussed herein, riblets have been used on aircraft as well as ships, yachts in particular. Garcia-Mayoral and Jimenez (2011) wrote a review on this subject, and that provides a starting point for interested parties. The fundamental manner in which the riblets affect friction drag was illuminated by Choi et al. (1993) who explained that the riblets disturb the usual streamwise vortices. The riblets' drawback is similar to that of roughness used in creating superhydrophobic surfaces in that as the spacing is increased, the effect is diminished. In fact, eventually they appear to the flow as roughness, which of course increases the friction.

Recently, Peet and Sagaut (2009) and Sasamori et al. (2014) conducted simulations and experiments, respectively, on sinusoidal-like riblets. Saravi and Cheng (2013) provide a review of FDR via riblets and textures in a turbulent flow. As a quick search on Google Scholar shows, research on riblets continues with about 40 references in the last two years alone. Only one of these references is mentioned herein as it approaches riblets from a material-choice viewpoint, and in so-doing is also a review of many of the investigations regarding riblets. West et al. (2016) review the changes in FDR that have been accomplished by different surface topographies and suggest that by varying material properties, additional drag reduction may be possible.

Compliant surfaces. The notion behind compliant surfaces reducing friction is that the deformation of the surface due to the presence of the turbulent boundary layer changes the adjacent flow in the inner region, this due to the compliant surface's believed viscoelastic properties. Riley et al. (1988) and Gad-el-Hak (2002) are review papers on this subject. Bandyopadhyay et al. (2005) reviewed earlier research and observed FDR to 17% for an axisymmetric body. As the surface loses its viscoelastic nature over time, FDR was seen to decrease. In a more recent paper that presents a framework for investigating compliant wall-turbulence interactions, and builds on previous work, McKeon and co-investigators (Luhar et al. 2015) provide a path forward for analysis of possible passive FDR over compliant surfaces.

Large-eddy breakup devices. By modifying the flow in the wake region, one can alter the friction along the solid surface, i.e. alter the velocity gradient in the inner region. In general, this mechanism to generate FDR is known as a Large Eddy Breakup Device. Spalart et al. (2006) advance that the structures affect the outer eddies and hence decrease friction drag. The issue is that while downstream (on the order of several boundary layer thicknesses) of

the devices there is a drag decrease of as much as 30%, the skin friction on the structures themselves may outweigh the benefits downstream. Park et al. (2011) conducted research on the spacing and sizes of these devices and realized a range of 5% to 9% FDR for the general results and the best case conditions, respectively.

Super-hydrophobic surfaces. One of the most recent and hence least studied techniques to reduce friction drag is the super-hydrophobic surface (SHS), which has been actively investigated for drag reduction for only about two decades. In fact these surfaces have many uses beyond those of FDR, and for example have been applied to help windshields whisk away rain, to windows and solar collectors to help them remain clean, and to fabrics to assist keeping them dry by repelling rain. As this is a relatively new methodology for FDR, which has been shown to work effectively in laminar flows, but much less so for turbulent flows, a larger discussion of this topic is requisite.

As is well-known, Navier proposed the concept of a “slip length”, which states that along a solid surface, the velocity gradient and the tangential velocity at the surface are proportional. In most instances, this has few consequences as regards continuum mechanics; however, this may be incorrect for a super-hydrophobic surface where a meaningful slip may be generated and thus a reduction in friction is realized. Rothstein (2010) gives a recent account of FDR via SHSs, which have been shown definitively for laminar flow, but less so for turbulent cases.

Here we review the work of Golovin et al. (2016) and Gose et al. (2016) who were funded by the Office of Naval Research under the same program. These investigators have shown definitively that SHSs can produce significant FDR in turbulent flow (to 50% for height-based Reynolds number ( $Re$ ) of 10000 to 40000), and are in the process of designing and

constructing more robust surfaces that generate FDR at even higher  $Re$ . In general, SHSs have surface roughness at the micro- and even nano-scales which entrap gas/air and is known as the Cassie-Baxter state, and thus cause slip. As long as the gas remains in these interstitial regions, and the roughness is not too large to appear as a rough surface to the liquid flow, FDR is realizable. If the gas-retaining roughness is too large, additional form drag is generated which overcomes the drag savings from the slip, and an increased friction is seen. Additionally, if the gas is lost due to turbulent pressure fluctuations which can drive gas from the roughness, a pressure decrease due to high-speed flow which can suck gas from the cavities, or due to diffusion of the gas from the roughness, the slip is lost, the surface state is known as Wenzel, and the friction increases. The interested reader is thus referred to these manuscripts. The outcomes of their investigations show that to achieve meaningful turbulent friction drag reduction, SHSs must have small feature size or  $k^+$  (defined as the physical roughness divided by the viscous length scale,  $l = \nu / u_\tau$  with  $u_\tau$  the friction velocity equal to  $\sqrt{\tau_{wall}/\rho}$  and  $\tau_{wall}$  the shear stress at the wall) less than one, and large high-pressure contact angles (and small contact-angle hysteresis). Note that previously,  $5 < k^+ < 9$  was considered hydraulically smooth. Other recent papers on SHSs include those of Srinivasan et al. (2015), Seo and Mani (2016) who discuss slip velocities in turbulent flow over SHSs, and Alame and Mahesh (2015) who conducted DNS of flow over super-hydrophobic grooves and its implications for drag reduction.

Surface coatings/paints Yang et al. (2014) developed a marine paint using a self-polishing copolymer anti-fouling paint mixed with polyethylene oxide (PEO), a well-known drag reducing polymer. In usual polymer injection studies many of which use PEO, hull penetrations are necessary. Although PEO has been shown to be very effective as a friction reducing agent (see below), the cost of storage, mix-

ing, and the hardware for injection including the hull penetrations, along with the cost of the polymer itself make it economically infeasible for surface ships (for one-time military operations, this is of course not an issue). Hence the purpose of this investigation was to explore the use of PEO infused marine paint to deliver the polymer. As compared to usual anti-fouling paint, in a water channel, the mixture reduced the friction by as much as 33% whereas in a tow tank, the reduction was a more modest 10%. As far as these coatings are concerned, the longevity issue is key, and the researchers conducted carefully-crafted experiments to uncover the PEO concentration as a function of time in a Couette-like rotor apparatus. The time rate of change of concentration was measured for a period of up to 3000 mins with water continuously supplied to facilitate a one hour residence time. Their results showed that the concentrations asymptotes at 3000 mins were similar to those required for appreciable friction drag reduction.

### 3.2 Active Methods; Polymer Injection

Numerous studies have now demonstrated the drag reducing benefits of polymers injected into the boundary layer (for a thorough discussion through 2015, see Perlin and Ceccio, 2015). Although there is no accepted theory of how polymers reduce boundary layer friction, there are two theories that are both based on the notion of polymer stretching. Regardless, there is an abundant literature on the subject of polymer drag reduction (PDR). Reviews proliferate including Lumley (1969); Liaw et al. (1971); Hoyt (1972); Virk (1975); Berman (1978); Sellin et al. (1982); McComb (1990); Nieuwstadt and Den Toonder (2001); and White and Mungal (2008). Generally, once a solvent/sea water is chosen/known and a polymer is selected, the most important parameters as shown by Virk (1975) are the concentration and molecular weight of the polymer. As they increase, the larger the friction drag reduction becomes until the maximum FDR asymptote is

reached. In the sub-sections that follow, a discussion is presented with more details of PDR.

Drag Reduction along a smooth wall To determine the relationship between polymer injection rate and persistence downstream, an investigation was conducted in the US Navy's Large Cavitation Channel. With  $Re$  to 220M through speeds to  $20 \text{ ms}^{-1}$ , Winkel et al. (2009) injected PEO and measured shear stresses with different molecular weights (nominally 2M, 4M, and 8M), concentrations (1000, 2000, and 4000 wppm), and varying rates of injection (to  $0.71 \text{ ls}^{-1} \text{ m}^{-1}$ ). These experiments had  $Re$  only one order of magnitude less than full scale. PDR of as high as 70% were realized, but this value decreased somewhat downstream due to degradation of the long chain polymers (this is shown in their Figure 17 as is the effects of roughness - see below). Myriad papers on this subject too numerous to mention are available (see Perlin and Ceccio (2015) for references).

Effect of roughness. To contrast the smooth wall effects just presented, similar experiments were conducted in the same facility with the same flat plate model along a surface that was purposely roughened with glass beads embedded in epoxy paint. This altered the  $k^+$  from 0.2 on the polished/smooth surface to about 400 on the roughened surface. The interested reader should consult the paper by Elbing et al. (2011). As is discussed below in the section on general roughness effects, and is expected, this shifted the turbulent boundary layer parallel to itself. In Fig. 6, the reproduction of their Figure 9, both smooth and rough wall friction drag reduction are presented. The PDR results along the rough surface show significant degradation in comparison, and are due likely to a combination of the following: (1) enhanced mixing leading to faster near-wall dilution; (2) a direct effect (i.e. a physical change caused by the roughness); and/or (3) a polymer degradation (chain scission) increase due to roughness.

Degradation. Degradation or scission of

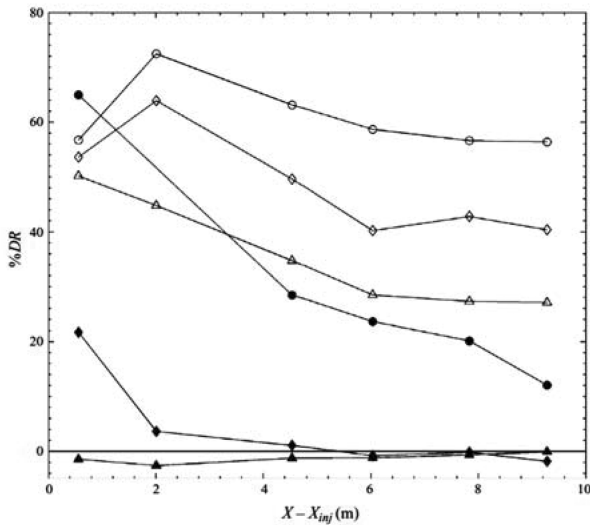


Figure 6 Reproduced from Elbing et al. 2011, their Figure 9 shows three speeds (6.8 (③), 13.5 (⑩), 20.1 (●)  $\text{ms}^{-1}$ ) with a direct comparison of the DR on the rough (solid symbols) and smooth (open symbols) surfaces as a function of distance downstream. The concentration of polymer injected was 4000 wppm, and the mass flux was at its highest

the long-chain polymer molecules can occur when they are stretched such as during pumping and injection, and also they degrade while awaiting use. As mentioned above, ideally one wants high concentration of large molecular-weight (MW) polymers for large friction drag reduction. However, although it may be cost effective to use high MW polymer with lower concentrations, for example, the larger the MW, the more easily a polymer undergoes scission. Once broken, the polymer essentially has reduced MW and hence reduced effectiveness (Patterson and Abernathy, 1970). Most of these investigations were focused on laminar flows, but in the study by Vanapalli et al. (2006) on turbulent flows, it was shown that degradation occurs at the Kolmogorov scales and a universal scaling was given. A later investigation was conducted by Elbing et al. (2009) to address the solvent issue and used PEO and PAM (polyacrylamide) solutes. Water and pseudo-seawater (a mixture prepared using Instant O-

cean) were used, and the universal scaling law of polymer scission (Vanapalli et al. 2006) was extended to greater Reynolds number. Hence it is clear that degradation issues are fundamental when considering PDR. Recently Pereira and Soares (2012) investigated the degradation of PEO and PAM polymers in a rheometer and proposed a degradation/decay model that predicts the drag reduction compared to its maximum value as a function of  $Re$ , concentration, temperature, and of course molecular weight.

**Cost benefit.** In most ship applications of FDR, the ultimate goal is to reduce the cost of powering the vessel, typically through fuel savings. For defense applications, increased speed may be the end game. For PDR, the cost of the injected polymer is an important consideration. Using various available data, it was possible to determine the quantity of polymer that must be injected to achieve a given reduction in skin friction. These data then were combined with estimates of powering efficiency, fuel cost, and polymer costs, to determine the financial breakeven point of PDR for a given set flow conditions (e.g. speed, vessel length, vessel surface roughness, etc.). Perlin, Ceccio and their collaborators (Perlin and Ceccio 2015) completed these calculations for a number of configurations, and the results suggest that the cost of the polymer will generally outweigh the savings due to reduced fuel consumption. This does not preclude the use of PDR when its implementation is for defense purposes or is meant to impact various aspects of vessel performance and operation through the intermittent reduction of friction drag. A text that discusses the economics of coatings (Marrion, Ed, 2004) such as anti-fouling coatings mentions application on ships (Milne, Chapter 1), although it does not specifically discuss them for polymer injection (drag reduction due to smoothness is mentioned).

### 3.3 Active Methods; Gas Injection

Bubble drag reduction Since McCormick

and Bhattacharyya (1973) seminal paper on using gas injection to generate FDR, myriad papers have been published. For review papers see Merkle and Deutsch (1992), Guin et al. (1996), Kato et al. (1998), Kodama et al. (2000), Moriguchi and Kato (2002), and Murai et al. (2007); a very recent review is presented in Murai (2014). The principal variables in BDR are the gas injection volumetric flow rate per unit span,  $q = Q_{\text{gas}}/l$ , the free-stream speed of the flow, the boundary layer thickness upstream of the injection location, and the stream-wise distance from the injector. In a series of publication on gas injection that generated bubbles (BDR) through air layers (ALDR), a group at the University of Michigan has published several important manuscripts. Sanders et al. (2006) reported on both FDR from gas injection and its downstream persistence. As they were the first group to have significant downstream distance to check the bubble persistence in reducing drag, they were the first to see a disturbing trend: despite the buoyancy of the bubbles, they were forced from the solid surface due to lift forces present, and BDR was essentially lost. For an up-to-date review article, see Hashim et al. (2015), which cites more than 100 publications on bubble drag reduction.

Air layer drag reduction It turns out that with sufficiently high gas injection rates, both the amount and persistence of FDR can be substantially increased. Elbing et al. (2008) showed that with increasing gas flux, the bubble flow associated with BDR transitions to a stratified gas layer. This air layer was quite stable and exhibited more than 95% friction drag reduction. Termed Air Layer Drag Reduction (ALDR), this method has been investigated frequently. In Elbing et al. (2013), the transition was studied again. The figure below presents the required gas flux for the transition from BDR to ALDR for smooth and fully rough surfaces. As is evident, the flux needed to achieve ALDR increases with increasing speed and with increased roughness. The approximate gas flux reported by Hoang et al. (2009) and

Mizokami et al. (2010) from sea trials are shown also, which shows that the gas fluxes used were sufficient to produce transitional or perhaps fully developed air layers. Hoang et al. (2009) measured 11% and 6% overall drag reduction for the ballast and full-load conditions, respectively (i.e. 7% and 4% energy savings) while Mizokami et al. (2010) reported energy savings of 8% to 12%. The economics of ALDR are discussed in Makiharju et al. (2012), who show that ALDR can be cost effective. The energy costs for pumping the air increases with increasing speed and draft, and decreases for increasing ship length. For a reasonably up-to-date review manuscript on ALDR, bubble injection cavitation, see Ceccio (2010).

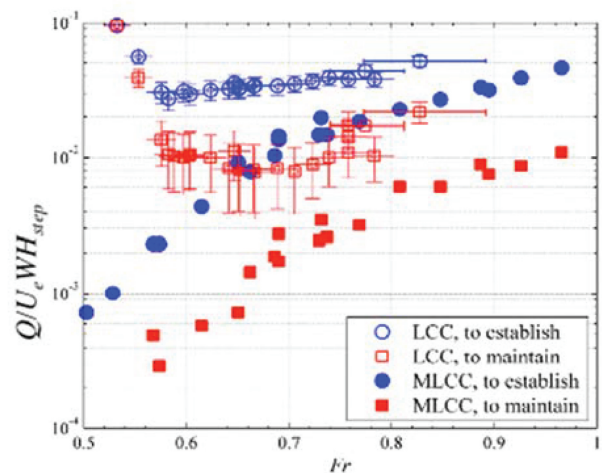


Figure 7 Air fluxes required for ALDR over rough and smooth surfaces (Elbing et al. 2008), where  $Q$  is the volume flux of injected gas per unit span beneath the bottom of a horizontal surface, and  $U_e$  is the free-stream speed. Data for smooth and fully rough surfaces are shown. These data are compared to the approximate air fluxes used in the sea trials reported by Hoang et al. (2009) and Mizokami et al. (2010)

Partial cavity drag reduction. Yet another technique used to reduce drag is the partial cavity where a separation between the TBL and the solid surface is produced through the application of air filled pockets. These cavities are

placed beneath the hull such that buoyancy will lead to capture of the gas and reattachment of the flow near the aft of the cavity. This so-called Partial Cavity Drag Reduction (PCDR) is discussed by Amromin and Mizine (2003), Matveev (2003), Lay et al. (2010), and Makiharju et al. (2013). Makiharju et al. (2013) compared PCDR on the same test model as the University of Michigan group used for BDR and ALDR. In this experiment, gas was injected behind a step and a wave-making gate was oscillated to perturb the flow to examine its influence on the cavity shape and air loss.

Figure 8 (reproduced from Figure 22 of Makiharju et al. 2013) exhibits the gas flux necessary to both establish and maintain a stable cavity as a function of flow speed, here shown as the Froude number  $Fr = U_c / \sqrt{gL}$ , where  $L$  is the cavity length. Experiments were performed in the Large Cavitation Channel and with a duplicate test model at 1/14 scale (ML-CC). In the large-scale experiment, roughly three times the gas flux was required to produce the cavity compared to the amount required to maintain it; the overall maintenance flux is reduced when the cavity reaches an optimal length. Observation of the small-scale model suggests that surface tension allows for lower maintenance gas fluxes at the lowest speeds; however, as the speed is increased, the non-dimensional gas flux begins to converge across a wide range of Reynolds numbers. An entire thesis focused on ship FDR (Zverkhovskiy 2014), which of course provides a recent, up-to-date literature review, also contains discussions of the author's experimental results, physics of cavities in steady flows, flat plate drag with cavities, and ship model experiments is available.

### 3.4 Other Active Methods

Surface Heating and Cooling. Two publications that examine surface heating and cooling in the context of FDR are presented by Yoon et al. (2006), and Kametani and Fukagata

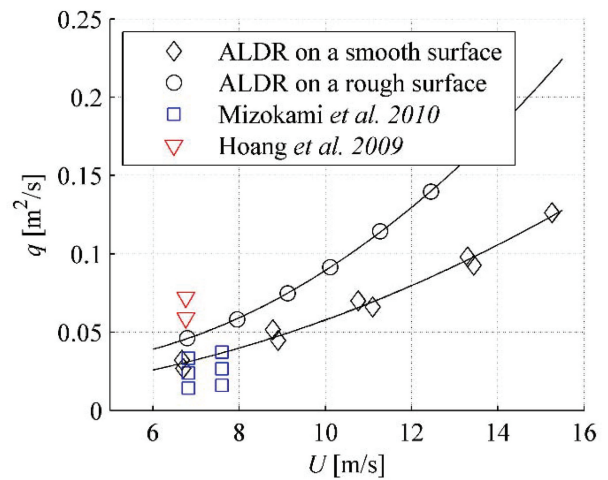


Figure 8 Non-dimensional critical gas flux to establish and maintain the cavities as a function of Froude number for the two scales: the Large Cavitation Channel (LCC) and the mini-Large Cavitation Channel (mL-CC)

(2012). Yoon et al. simulate the flow over periodically heated and cooled surfaces with Reynolds numbers of about 2000 and Grashof numbers between  $10^6$  and  $10^7$ . They found friction drag reduction as large as 35% due to buoyancy effects alone. Simulations show that the lateral motions generated by the buoyancy help destroy the coherent structures, and therefore decrease skin-friction drag. In Kametani and Fukagata (2012), the authors simulate both uniform cooling and uniform heating of the surface, and investigate the resulting flows systematically for Richardson numbers varying from  $-0.1$  to  $0.1$ . Although uniform heating caused an increase in friction, uniform cooling reduced the near wall Reynolds stresses and led to drag reduction of to 65%. While these large reductions appear attractive, the net energy savings are questionable.

Electromotive force. Numerical simulations indicate that electromotive / Lorentz forces can be used for drag reduction; however as with the heating and cooling, it is the net energy savings that remain a major challenge. Recent reviews are available in the publications by Berger et al. (2000) and Mamori and Fuka-

gata (2011). In Berger et al., the authors use alternating strips of electrodes and magnets and simulate the application of Lorentz forces. These electromotive forces act at right angles to the flow, and both open and closed loop control is implemented. They realize large friction drag reduction to 40%. Regrettably, their own energy requirements are an order of magnitude larger than the energy savings due to skin-friction reduction. Mamori and Fukagata (2011) applied a sinusoidal profile of a wall-normal Lorentz force to the flow, and show that this standing wave can suppress the formation of streamwise vorticity in the near wall region.

Mass blowing and suction. Blowing and suction have been topics of significant interest, especially as regards their effect on skin friction. Simpson et al. (1969) studied this for large area blowing and suction. Antonia et al. (1995) discuss the effect of blowing and suction over small areas and their effect on friction downstream. Additionally many other studies show that mass addition can significantly disrupt the momentum profile of the inner flow and lead to significant changes in skin friction. Subsequently, investigators have implemented “net-zero flux” mass injection to modify skin friction; see Bewley et al. (2004). They suggested that the skin friction could be reduced to the equivalent of a laminar flow, the lower bound of possible FDR. Min et al. (2006) also did research in this area and somewhat surprisingly showed that it may be possible to reduce the skin friction to a value less than that of laminar channel flow by generating negative Reynolds stresses via controlled blowing and suction that create an upstream travelling wave. In a more recent paper by Fukagata and co-workers (Kametani et al., 2015), a discussion of uniform blowing and suction in a turbulent flow is offered. The authors have provided a detailed description of the attendant physics seen with their LES simulations having realized about a 10% FDR via this technique.

Wall motion and deformation Controlled

motion of the solid surface can disturb the near-wall momentum and change FDR as shown experimentally by Choi et al. (1998) and computationally by Baron and Quadrio (1996); FDR as high as 40% was achieved. For fully-developed channel flows Fukagata (2011) reviewed passive and active drag reduction using numerical simulations of wavy surfaces for the suppression of Reynolds stresses. Fukagata (2011) stated that passive techniques were inconclusive as far as drag reduction effectiveness was concerned. Furthermore, he found drag reduction to 8% using active streamwise traveling waves, which also can be responsible for a drag increase. As with all these other methods, the issue of net energy savings is the concern. Tomiyama and Fukagata (2013) investigated this phenomenon via direct numerical simulation. They numerically realize a net energy savings as large as 12.2%. Physical experiments conducted by Itoh et al. (2006) and Tamano and Itoh (2012) have demonstrated drag reduction of roughly 10% as a consequence of spanwise traveling waves (on zero-pressure gradient turbulent flows). As with many of the aforementioned techniques, there has been tremendous interest in using wall motions to reduce friction drag, and recent publications include Lardeau and Leschziner (2013), Yakeno et al. (2014), Skote (2014), Agostini et al. (2014) and Li et al. (2015).

### 3.5 Roughness Effects: Review of Turbulent Boundary Layers without and with Roughness

Roughness, random or patterned, distributed on the surface over which liquid flows will likely alter the flow as compared to a smooth solid surface. In the case where the roughness is much smaller than the sublayer, it has no effect and the surface is known as hydraulically smooth. (See the section: Passive Methods - Super-hydrophobic surfaces for a discussion of roughness in those cases.) When roughness elements protrude into the buffer layer, they may interrupt the viscous sublayer and cause a form

drag, which increases the total drag above its smooth-wall level. In this situation,  $\tau_w$  depends on the dynamic viscosity  $\mu$  and the roughness  $k$ , and the surface is termed transitionally rough. When roughness elements extend further into the boundary layer disturbing the buffer layer as well,  $\tau_w$  loses its dependence on  $\mu$  and the surface is termed fully rough. In this case, shear stress is transmitted to the solid surface by the form drag on the roughness features.

The first quantitative work on turbulent flow along rough surfaces and its effect on friction was conducted by Nikuradse (1933). He studied how uniform-size sand-grain roughness affected pipe flow friction. This effort is still highly regarded and as a consequence, equivalent sand-grain roughness is still used as a roughness measure. If the physical roughness is given by  $k_s$ , and non-dimensionalizing by the viscous length scale, we have  $k_s^+ = k_s/l_v$ . Using this non-dimensional roughness, the following is historically considered as the approximate divisions between the three regimes: Hydraulically smooth  $k_s^+ < 4$ ; transitionally rough  $4 < k_s^+ < 70$ , and fully rough  $70 < k_s^+$  (Note that these are different for SHS FDR).

For transitionally-and fully-rough TBL flows, the mean streamwise velocity profile is well-represented by the usual log law modified to include a downward vertical shift  $\Delta U^+$  known as the roughness function:

$$U^+ = \frac{1}{\kappa} \ln(y^+) + B - \Delta U^+ \quad (1)$$

Here  $\kappa$  is known as the von Karman constant and B as the wall offset. Nikuradse's study set forth a fundamental understanding between random roughness and turbulent flow; however, recently investigators believe that 2D, random, and other surfaces may generate slight differences in flow alteration (Jimenez, 2004; Flack and Schultz, 2010, 2014; and Andrewartha et al., 2010). In fact, most investigators have

found that the increase in frictional resistance due to roughness is due to a corresponding increase in the wall shear stress  $\tau_w$ , rather than a fundamental change in flow structure (Flack and Schultz, 2014).

#### Structured 2D, 3D and random roughness.

As mentioned above, the roughness effect on the mean flow can be well-represented by using the  $\Delta U^+$  term in the log-law; however, the value of this term is not known even if the roughness topography is well-characterized - that is, direct measurements are required to quantify the offset's value, and this makes its use difficult. (Flack and Schultz, 2010 provide roughness correlations, but a suitable correlation for general, expansive roughness is elusive.) Therefore, the prediction of the mean flow from measurements of surface roughness topography remains.

The characteristics of the motions in the flow above rough surfaces is difficult to determine as is obvious that flow is highly dependent on the specific geometry of the surface roughness. An obvious parameter of interest is the mean spacing between individual roughness elements which may be described by the so-called solidity  $\lambda$ , which compares the total projected frontal area to the wall parallel projected area of the elements. Experiments have demonstrated that for values lower than  $\lambda \approx 0.15$ , the effect of roughness increases with solidity; on the other hand, values greater than  $\lambda \approx 0.15$  show a decrease as roughness elements begin to shelter each other from the flow (Jimenez, 2004). These two regimes essentially represent driven-cavity flows and blockage type flows, respectively. Limited data from studies of surfaces with narrow, transverse grooves suggest that the equivalent roughness height  $k_s$ , may scale with the boundary layer thickness  $\delta$  (Perry, Schofield and Joubert, 1969). Therefore, roughness may be distinguished as 'd-type' scaling, which scales with the boundary layer thickness or 'k-type' scaling, which scales with roughness height.

Perhaps the most disputed idea in studies of turbulent flow over rough surfaces is the concept of wall similarity, an extension of Townsend's (1976) Reynolds number similarity hypothesis. This states that for high Reynolds number flows, turbulent motions are independent of wall roughness and viscosity outside the roughness sublayer (Schultz and Flack, 2007). Here Schultz and Flack define the roughness sublayer as the region of flow extending about  $5k$  into the flow. What happens in the outer layer over that seen along a smooth, flat plate is still a point of contention.

As detailed in Volino et al. (2011), several studies have sought to validate wall similarity. Recent experimental work by Kunkel and Marusic (2006), Flack et al. (2005) and Flack and Schultz (2014) all support wall similarity for both mean flow and Reynolds stresses, while the investigations of Krogstad et al. (1992), Tachie, Bergstrom and Balachandar (2000) and Keirsbulck et al. (2002) all present Reynolds stresses that are altered in the outer flow. Numerical simulations by Leonardi et al. (2003) and Bhaganagar et al. (2004) also question the assertion that wall similarity holds. In a review of the topic of turbulent flow over rough walls, Jimenez argued that researchers need consider the blockage ratio of the boundary layer thickness to roughness height  $\delta/k$  (Jimenez, 2004). He maintained that values of  $\delta/k$  must be greater than  $\sim 40$ -80 before the outer layer flow is unaffected by roughness effects. Analysis by Flack and Schultz of their data leads them to conclude that wall similarity holds for all 3D roughness. And for 2D roughness, they maintain that for sufficiently-high Reynolds number and  $\delta/k$ , wall similarity likely holds as well.

### 3.6 Biofilms, Biofouling and Mitigation by Anti-fouling Coatings

It has been long-known that marine fouling leads to increased drag; however, the underlying physics associated with this phenome-

non remain murky. This fact was responsible for engineers pursuing coatings to mitigate the accompanying drag penalty. The most powerful and effective anti-fouling coatings were made of tributyltin, which prevented the growth of most types of biofouling, although they are not able to entirely prevent 'slime layers' have been banned by the International Maritime Organization (IMO) as a consequence of their environmental impact (Schultz, 2004).

Various anti-fouling (AF) coatings and timely cleaning have proven effective in managing macrofouling (e.g. barnacles, muscles, etc.); however, microfouling (defined as a biofilm or a 'slime layer' such as colonies of bacteria, diatoms and algae) remains a major source of increased skin friction on ships. Microfouling develops rapidly on ship hulls, and worse, several biofilms persist under even the strongest AF coatings (Schultz and Swain 1999). The detrimental effects of increased skin friction are obvious. Ship trials performed by Haslbeck and Bohlander (1992) demonstrated that a KNOX class frigate required roughly 18% less shaft horsepower to cruise at a speed of 25 knots, and likewise increased its maximum speed by one knot following a hull cleaning of a biofilm layer.

In the 1980s, the penalties associated with microfouling on ship hulls, and on the transportation industry as a whole, led to increased interest in the hydrodynamic effects of biofilm layers. Picologlou et al. (1980) investigated microbial slime layers in pipes, identifying the importance of the interaction between the biofilm and hydraulic flow, both as regards slime layer formation and energy dissipation. The authors also noted that when present thin filaments in the biofilm appeared to be responsible for additional energy dissipation. Lewkowicz and Das (1981) studied nylon tufts attached to a rough plate to simulate marine slime growth and their results not only supported the notion of an increase in skin friction, but also included velocity measurements of the mean flow and

turbulent statistics. Recently, several comprehensive investigations of flows over biofilm have been undertaken. Both Schultz (1998) and Andrewartha (2010) investigated flow over biofilm layers in their doctoral work. Both recorded point measurements of the velocity field over biofilms using Laser Doppler Velocimetry (LDV). As expected, both researchers found an increase in the friction coefficient for plates when covered in biofilm.

## 4 SURVEY OF ENERGY SAVING METHODS

### 4.1 Categorization of Energy Saving Methods

So far, many works to review and categorize energy saving devices have been conducted. For instance, in the 22nd ITTC, the Specialist Committee on Unconventional Propulsors made a great effort to categorize the energy saving devices. In the report, at first the devices are categorized from the viewpoint of recovery of rotational wake energy. The typical devices are vane and fin. These devices are categorized into three types: location of devices before propeller, after propeller and both. Next they investigated ducted propulsor, today widely used as an ESD (Energy Saving Devices). In the 27th ITTC Resistance Committee, the air lubrication method is reviewed as a new technology, and the activity in Japan is introduced. Also in the 27th ITTC Propulsion Committee, a contra-rotating propeller (CRP) with pod propulsor system, a rudder pod system, and an electric-run CRP system are reviewed. The committee also reviewed many types of ESDs such as pre-swirl devices, post-swirl devices and so

on. As the previous reviews were conducted in a very systematic manner, it is very helpful to review again the energy saving devices. However, in the present committee, the theme is widened, from energy saving devices to energy saving methods; hence we have to alter the category table to cover the energy saving methods. As the energy saving methods are conceptually broad, it is not easy to tabulate the energy saving methods. There are various viewpoints, e.g. physical mechanisms of energy saving, location of the devices and so on. In this committee, we first categorize the energy saving methods by 'Principle'. Each energy saving device has its principle as to why the energy saving occurs. For instance, some devices reduce frictional drag directly, while some recover the rotating motion which is generated by the propeller, and so forth. Here we set four principles. They are 'Direct drag reduction', 'Reducing propulsive losses', 'Use of renewable energy' and 'Operation'. The category 'Operation' has not been included as an ordinary energy saving device, but it would be included as energy saving methods or measures. Under each principle, sub categories are established. For instance, under 'Direct drag reduction', we categorize the drag component we aim to reduce. They are categorised as 'Mechanism'. Under each mechanism, the 'Technique' is the element of the next category. Finally, under each technique, more specific 'Methodologies' are listed as the last category. Table 2 is the categorized table of energy saving methods. In the table, the percentage of energy-saving rate for each method is not presented, contrary to the previous categorization. This is because the energy-saving rate may have large variance and it is not straightforward to determine a precise value.

**Table 2 Categories of energy saving methods**

Principle	Mechanism	Technique	Methodology				
Direct drag reduction	Frictional resistance	Wetted surface area	Air lubrication				
		Reduce shear force	Low friction paint				
	Viscous pressure resistance	Boundary layer control	Generate local vortices	Constrain flow via a duct			
			Hull optimisation				
	Wave-making resistance	Bow shaping	Bulbous bow	Hull optimisation			
	Aero drag reduction	Shaping of upper structures	Corner rounding	Downsizing of upper structure			
			Bow shaping	Hull shape			
	Added wave resistance	Incident wave reflection					
Ship motion							
Reducing propulsive losses	Relative rotative efficiency	Bilge vortex energy recovery	Pre swirl stators				
			Vortex generators				
	Hull efficiency	Hull-propeller interaction	Vortex generators	Hull-propeller optimisation			
			Rotational efficiency	Reduce rotational energy in the propeller wake	Pre swirl stators	Contra-rotating propeller	
	Reaction rudder	Rudder fin					
	Hub fins	Overlapping propellers					
	Axial efficiency	Hub vortex recovery			Hub fins	Rudder bulb	
					Reduce tip vortex	Tip-fin propeller	Tip-rake propeller
						In-flow management	Ducts
	Frictional efficiency	Coatings		Low friction paint			
		Boundary Layer control		Injection			
	Propeller design	Blade design		Area, thickness, section, tip loaded propeller			
		CFD, optimization					



Principle	Mechanism	Technique	Methodology
Use of renewable energy	Wave	Lifting surface in waves	Forebody fin
	Wind energy	Additional thrust	Sails
			Kite
			Flettner rotor
Solar energy	Electricity generation	Photovoltaic panels	
Operation	Optimisation in operation	ICT	Weather routing
			Slow steaming
	Aging	Maintenance	Docking
			Roughness treatment

## 4.2 Review of Recent Research on ESM

In this section, recent work related to the energy saving methods are reviewed. The conferences we reviewed over the period 2013-2016 were:

- Advanced Model Measurement (AMT)
  - 17-18 September (2013), Gdansk, Poland
  - 28-30 September (2015), Istanbul, Turkey
- CWT2015 : Tokyo 2015 A Workshop on CFD in Ship Hydrodynamics, 2-4 December (2015), Tokyo, Japan
- Compit: Conference on Computer and IT Applications in the Maritime Industries
  - 15-17 April (2013), Cortona, Italy
  - 12-14 May (2014), Redworth, UK
- EDRFCM 2015 : European Drag Reduction and Flow Control Meeting, 23-26 March (2015), Cambridge, UK
- IMAM 2015: International Maritime Association of the Mediterranean, 21-24 September (2015), Pula, Croatia
- ISOPE: International Ocean and Polar Engineering Conference
  - 15-20 June (2014), Busan, Korea
  - 21-26 June (2015), Kona, Hawaii, USA
  - 26 June-1 July (2016), Rhodes, Greece
- IWSH: International Workshop on Ship and Marine Hydrodynamics
  - 23-25 September (2013), Seoul, Korea
  - 26-28 August (2015), Glasgow, UK
- JMST : Journal of Marine Science and Technology, issued from 2013 to 2016.
- JSR : Journal of Ship Research, issued from 2013 to 2016.
- MARINE: International Conference on Computational Methods in Marine Engineering
  - 29-31 May (2013), Hamburg, Germany
  - 15-17 June (2015), Rome, Italy
- MARSIM 2015 : International Conference on Ship Manoeuvrability and Maritime Simulation, 8-11 September (2015) Newcastle, UK
- NAV 2015 : 18th International Conference of Ships and Shipping Research, 24-26 June

(2015), Lecco, Italy

- NuTTS: Numerical Towing Tank Symposium
  - 2-4 September (2013), Mülheim, Germany
  - 28-30 September (2014), Marstrand, Sweden
  - 28-30 September (2015) Cortona, Italy
  - 3-4 October (2016) St Pierre d'Oléron, France
- Ocean Eng. : Ocean Engineering an International Journal of Research and Development
- PRADS: International Symposium on Practical Design of Ships and Other Floating Structures
  - 20-25 October (2013), Changwon, Korea
  - 4-8 September (2016), Copenhagen, Denmark
- RINA EES 2015 : 4th RINA Energy Efficient Ships, 4 November (2015), Rotterdam, The Netherlands
- SMP: International Symposium on Marine Propulsors
  - 5-8 May (2013), Launceston, Australia
  - 1-3 June (2015), Austin, USA
- SNH : Symposium on Naval Hydrodynamics
  - 30th SNH, 2-7 November (2014), Hobart, Australia
  - 31st SNH, 11-16 September (2016), Monterey, USA

## 4.3 Direct Drag Reduction

Paint/Fouling/Roughness/Compliant Coating. Low frictional paints have interested naval architects who seek the ship drag reduction. In some journals and conferences, many researchers have carried out studies to clarify the mechanism of frictional drag reduction by use of low friction paint, anti-fouling paint and slime. Here, some works are reviewed. Lee et al. [2013] propose laboratory standard procedures for the performance evaluation of low frictional anti-fouling marine paints. Paik et al. [2013] introduce the flat plate model test method in cavitation tunnels to evaluate the skin friction of the marine coating or treated-surface. They also

demonstrate the Laser Doppler velocimetry (LDV) technique to evaluate the drag and to determine the reason for the drag reduction. Walker et al. [2014] research skin friction for anti-fouling coating surfaces and show that the fouling release surfaces have lower frictional drag compared with anti-fouling surfaces. They also evaluate the drag reduction due to anti-fouling surfaces at full-scale. Yang et al. [2014] develop a skin-friction reducing marine paint by mixing fine powder of PolyEthyleneOxide with self-polishing co-polymer and anti-fouling paint. Results of drag reduction experiments are also presented. To clarify the mechanism of drag reduction due to slime, Newcastle University has conducted several experiments. Atlar et al. [2015] describe the design, manufacture and operation of a specially designed strut arrangement deployed on a research vessel to carry a number of standard test panels to collect dynamically grown, natural slime while the vessel is in-service. Although research on compliant coatings has been inactive recently, Schrader et al. [2015] conducted such an experiment to evaluate the drag reduction for compliant coatings. As one of the candidates for compliant coatings, the bow of a search-and-rescue boat was introduced. The experiment was done at high-speed in a circular water channel. Paik et al. [2015] investigated the drag reduction for anti-fouling paints, one was a silicon-type self-polishing co-polymer (SPC), and the other was conventional SPC. They showed that the better drag performance is obtained for silicon-type SPC in the high speed region. Tamano et al. [2015] proposed a new drag-reducing method using an electrostatic flocking surface with grooves, and carry out the experiments using a small circular channel. Lee et al. [2015] introduced a new drag reduction coating material, FDR-SPC (Frictional Drag Reduction Self-Polishing Co-Polymer) with PEGMA (Poly-Ethylene Glycol Methacrylate). Kulik et al. [2015] studied compliant coatings for frictional drag reduction on a flat plate. As basic research investigating skin friction, Yeginbayeva et al. [2016] investigated the combined effects of sur-

face roughness and a biofilm, which is grown on a marine research vessel and under controlled laboratory conditions in a “slime farm”.

Super-Hydrophobic Surfaces (SHS). Super-hydrophobic surfaces (SHS) represent another candidate for frictional drag reduction and much research concerning this theme has been carried out. For instance, Seo et al. [2014] simulated the turbulent flow textured SHSs using Direct Numerical Simulation (DNS) and discuss the possibility of drag reduction. Srinivasan et al. [2015] studied the drag reduction due to depositing sprayable super-hydrophobic microstructures on the inner rotor surface of a rotating device, a Taylor-Couette rheometer. Zhang et al. [2016] investigated the drag reduction of SHSs using a rectangular water channel made with super-hydrophobic upper and lower surfaces, and study the mechanism of drag reduction. Golovin et al. [2016] comprehensively review the drag reduction due to SHSs, including wettability, roughness and scaling laws. In the 31st SNH (Symposium on Naval Hydrodynamics) [2016], research on drag reduction due to SHSs are discussed. Du et al. [2017] show a method to maintain the air layer on the hydrophobic surface by combining air injection and surface hydrophobicity adjustment. Due to the slip effect, a drag reduction up to 20% is obtained.

Air Lubrication. In the 27th ITTC Resistance Committee, air lubrication methods are already reviewed as new technologies. Hence only the work after the 27th Resistance Committee’s review are introduced. Kamiirisa et al. [2015] reviews the recent activities on air lubrication methods in Japan. Several types of actual (commercially used) ships are selected, which include a training ship, a cement carrier, a product carrier, a bulk carrier and a car ferry. Except for the ferry and training ship, the test ships are selected such that the bottoms are wide and flat. As ship size increases, the energy required to inject air bubbles to the ship bottom becomes larger. This fact is a large det-

riment to the air lubrication method on ships. To overcome this problem, a new air injection system is proposed. In this system, scavenged air from the diesel engine is extracted to inject air beneath the ship. As scavenged air has very high pressure and no contaminants, this method seems to be promising as a new air injection supply.

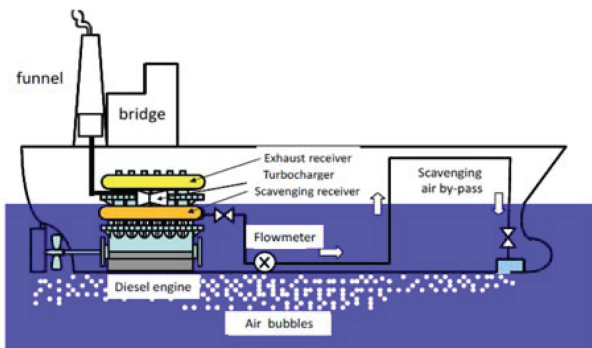


Figure 9 Application of scavenging gas from the main engine to provide air lubrication, Kamiirisa et al. [2015]

Air-lubrication researches are carried out in other countries in addition. These include Jang et al. [2013], which carried out an experiment of drag reduction of a model ship using air lubrication; and Zverkhovskiy et al. [2013], which describe the experimental study of the frictional drag reduction on a horizontal flat plate by an air cavity in a cavitation tunnel. Furthermore, Zverkhovskiy et al. [2014] conducted an experiment on drag reduction via an air-cavity method on the bottom surface of the hull. Herein, the ship model used was an inland waterway ship. They also discussed the stability of the air cavity. Jagdish et al. [2014] experimentally investigated the sustainability of an air layer aimed at frictional drag reduction. Slyozkin et al. [2014] carry out an experiment of drag reduction by an air-layer over a flat plate in a cavitation tunnel, and show details of the experiments and results. Pang et al. [2014] simulated turbulent flows with microbubbles by use of DNS (Direct Numerical Simulation) with two-way coupling and discuss the mechanism of drag reduction. A multi-phase Lagrangian and Eulerian model is used in the simulation.

Butterworth et al. [2015] carry out drag reduction experiments for an air cavity system applied to a container ship and show results of their experiments. In their work, seakeeping tests are also included. Agrusta et al. [2015] carry out an experiment of drag reduction for a high-speed boat wherein air is ventilated into the ship bottom. Silberschmidt [2015] reports the result of a sea trial test for a 40,000 DWT tanker which is equipped with an air lubrication system. Park et al. [2016] carry out an experiment using air lubrication applied to a tanker ship model, and show the trajectory of air bubbles around the ship bottom as well as resistance curves under air lubrication.

Wave load. Contrivances to reduce the added resistance of ships in waves are one of many methods to save energy. Kuroda et al. [2013] showed the effectiveness of STEP, retrofitted type incident wave breaker to reduce the added wave resistance. They presented the model test result and improvements in the full-scale ship case, too. Sakurada et al. [2016] developed a new ship bow form above the waterline called COVE to reduce added resistance in waves and demonstrate the effect through experiment and theoretical calculation. Jung et al. [2016] studied ship performance in waves and a new concept of hull-form design including the effects of added resistance. They introduced some examples of the sensitivity analysis of added resistance and the weather factor to the variations of ship dimensions. Lee et al. [2016] investigated three different bow shapes for a VLCC to reduce added resistance in waves. In the study, both full load and ballast conditions are considered. On the other hand, Hwang et al. [2016] studied two different bow shapes for mega container ship in waves.

Design/Optimization. In this committee, the design of hull and hull-propeller systems to get optimum propulsive efficiency is temporarily categorised under “Direct drag reduction”. Recently as the performance of computers has improved, many researches on the design opti-

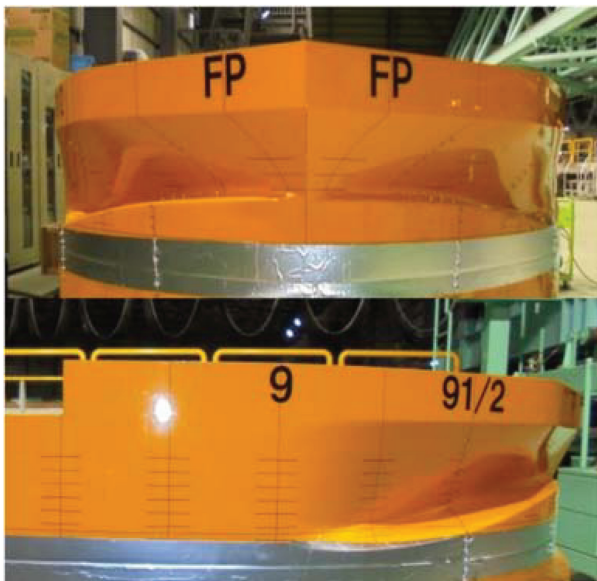


Figure 10 COVE, Sakurada et al. [2016]

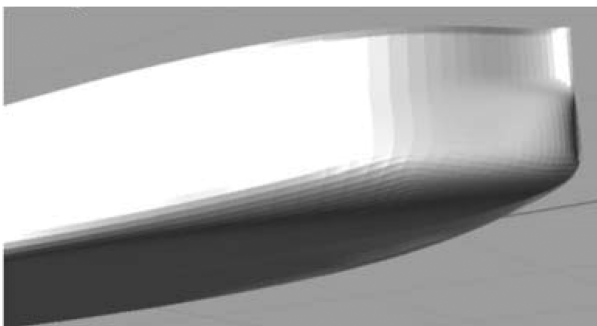


Figure 11 Hi-Bow, Lee et al. [2016]

mization of hull shape have been carried out. Here typical works are reviewed. Ginnis et al. [2013] demonstrated the multi-objective optimization for the bow shape of a container ship based on a BEM solver. Hochkirch et al. [2013] studied the hull optimization for a large container ship, not from the viewpoint of a single design point, but over the whole operational range, and they demonstrate the reduction of fuel consumption. Hansen et al. [2013] introduced a design system ECO-product to optimize trim condition for energy saving. Hochkirch et al. [2013] broadly discussed the difference between full-scale and model-scale flows on hull optimization and trim optimization. Dong et al. [2014] and Shen et al. [2014] carried out hull form optimization using the radial

basis function (RBF) method. Li et al. [2014] studied hull form optimization for a bulk carrier considering total ship resistance and the quality of the wake at the propeller plane as objective functions. Dang et al. [2015] apply the concept of an asymmetric aftbody to improve propulsive performance. They used a Reynolds Averaged Navier-Stokes (RANS) solver to evaluate the viscous flow field around the ship while the propeller performance is estimated by a potential flow based boundary element method. They obtain an asymmetric aftbody whose propulsive performance is better than a symmetric aftbody. Campana et al. [2015] propose an efficient hull optimization method under the uncertainty of ships operating in a real scenario. A study by Kim et al. [2015] investigates the hull optimization technique using parametric modification functions and particle swarm optimization. They also show the result of the multi-objective problem. In the MARINE 2015 conference, several works on the ship hull optimization are introduced. For instance, Bertram et al. [2015] review the optimization of a ship hull, using a full-scale free-surface RANS simulation. Furthermore, trim optimization is discussed. Brenner et al. [2015] studied optimization using the concept of “design velocity” and “adjoint shape sensitive”. Van der Ploeg [2015] studied the optimization of an aftbody to minimise power and obtain the best wake field, considering full-scale effects. Scholcz et al. [2015] studied meta-modelling for efficient multi-objective optimization of hull forms.

Tahara et al. [2016] showed a multi-objective design optimization for the determination of the stern form and pre-swirl duct shape. Diez et al. [2016] presented a method to reduce the dimension of design spaces in hydrodynamic shape optimization. They applied a Karhunen-Loeve expansion to a combined geometry and physics based design modification vector. Chang et al. [2016] studied an efficient hull optimization method based on an approximate model and sample selection method. Kleinsorge

et al. [2016] demonstrated the hull form optimization considering a number of most probable upcoming operating conditions which are forecasted by a scenario program.

**Air Drag.** Air drag acting on a ship above its waterline is another target to reduce total ship resistance. Ouchi et al. [2015] propose a new windshield on the bow of a container ship. They carry out model experiments in a wind tunnel and equip it with a new windshield on a 6,700TEU container ship. Kim et al. [2015] investigate air drag contributions of each part of the superstructure and containers of a container ship through the use of RANS simulations. They also estimate the efficiencies of shape modification and add-on devices on the superstructure and containers on the air drag reduction. He et al. [2016] investigated the reduction of air resistance acting on a ship by using interaction effects between the ship hull and its accommodation. Three types of accommodation box type, plate type and streamline type are studied through CFD, see Figure 12 for the streamlined accommodation.

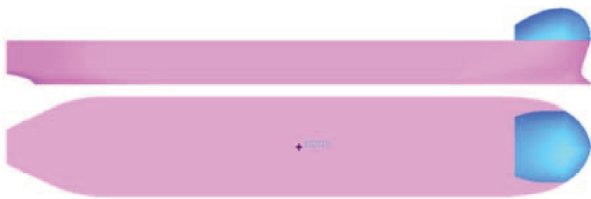


Figure 12 Ship hull and streamlined accommodation to reduce air drag, He et al. [2016]

#### 4.4 Reducing Propulsive Losses

**Duct.** The history of ducts used as energy saving devices is long and to date, much research related to ducts have been conducted. Here typical recent efforts are reviewed. Gaggero et al. [2013 SMP' 13] carry out the optimization of a decelerating ducted propeller and the results obtained are compared with experiment. Rao et al. [2013] show a numerical method to evaluate the propeller force on a ducted

propeller with pre-swirl stator equipped in the duct. Guiard et al. [2013] introduce a new concept of a pre-swirl duct for a high-speed vessel, called the Becker twisted duct (BTD). Yuhai et al. [2013] carry out CFD simulations for a VL-CC with pre-swirl symmetric and non-symmetric ducts and the wake at the propeller plane is discussed. Sakamoto et al. [2014] numerically simulate a Panamax bulker with duct by solving RANS equations. They simulated the propulsive performance with and without a duct in the model and at full scale, and the scale effect is discussed. Lee et al. [2015] directly measured the force acting on the model of an asymmetric duct. Such experimental data should give us important information for CFD validation. Bhattacharyya et al. [2015] carry out research on the scale effect of a ducted, controllable-pitch propeller via CFD. Rueda et al. [2015] optimize the ship stern form considering the duct effect to maximize energy efficiency.

To provide a set of benchmark data for duct, the National Maritime Research Institute (NMRI) planned a CFD workshop [Tokyo 2015 A Workshop on CFD in Ship Hydrodynamics] and offered the dataset of measured velocity using PIV obtained by NMRI and Osaka University. In the workshop, many researchers participated and presented their results. These results should be helpful as for validation of future numerical research.

Hori et al. [2016] measured the stern flow with a duct and with/without the propeller effect using SPIV, and they obtained validation data for CFD. Ichinose et al. [2016] proposed a new concept of duct called 'USTD' which is a small duct 'WAD' equipped on a V-type ship hull. The performance of a USTD is evaluated through CFD simulation. Go et al. [2017] studied the effect of a duct before a propeller on the propulsive performance. The duct diameter and the attack angle of the duct are parametrically changed, and the propulsive performance in open water conditions are investigated using numerical simulation. Figure 13 exhibits

the streamlines found by Nishikawa [2015].

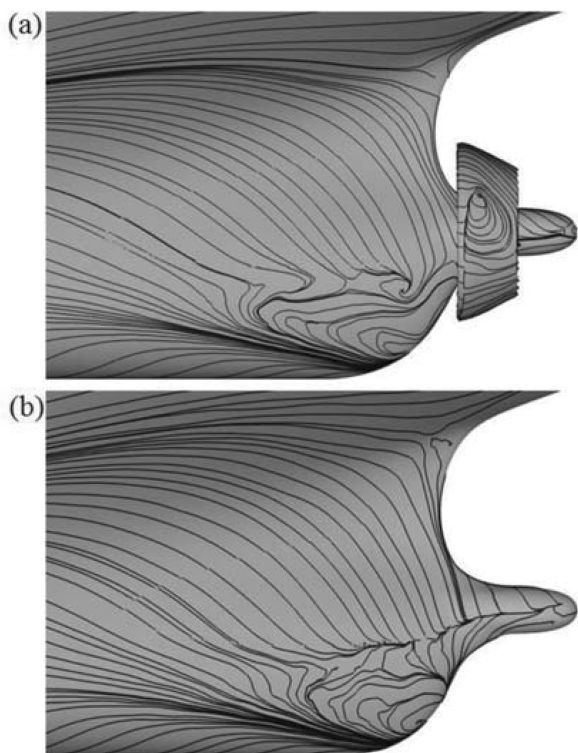


Figure 13 LES limiting streamlines on a Japan bulk carrier: duct equipped (upper), no duct (lower), result obtained by Nishikawa [2015]

Pre-swirl devices. Research on pre-swirl devices such as stator fins also has been carried out by many researchers. Schuiling [2013] studied a new type of ESD, called BSD, a combination of pre-swirl stators and duct. Brenner et al. [2013] studied the optimization of a retrofit-type fin ESD using a CAD and CFD system. Hsieh et al. [2013] precisely analysed the flow with and without an asymmetric pre-swirl stator by use of CFD. They focused on the energy-loss with/without ESD to clarify the energy saving mechanism. Kim et al. [2014] investigated the scale effect for pre-swirl type energy saving devices such as a duct and a duct with pre-swirl stator fins using CFD. They showed that the performance of energy saving devices reduces as the Reynolds number increases.

Bugalski et al. [2014] studied the propeller

induced pressure pulse on the hull with several types of ESD, including a pre-swirl hull fin (vortex generator), a boundary layer alignment device and a pre-swirl stator. They simulated the pressure pulse using an in-house code based on deformable lifting surface theory. Numerical results are compared with experiment. Park et al. [2014] discuss the asymmetric pre-swirl stator using CFD simulation. They investigated an asymmetric pre-swirl stator at full scale as well as at model scale and show that the performance reduces in full scale. Yan et al. [2015] designed asymmetric pre-swirl stators by QCM and CFD. They also analysed the performance of stators at full scale. They showed a power savings with and without ESD via sea trials. Park et al. [2015] simulate a full-scale wake with and without pre-swirl stators-equipped ships and show the difference of the wake at the propeller plane. Bensow [2015] investigated the hull-propeller interaction with pre-swirl stators using Large Eddy Simulation (LES). Furthermore, in their work, cavitation and no-cavitation conditions are considered. Lee et al. [2015] present the results of development and application of an ESD, which is a simple fin-shaped appendage attached to the stern bilge area. To verify the performance of this ESD at full scale, sea trial tests are performed for a series of 35K bulk carriers. Streckwall et al. [2015] numerically studied the scale effect of a stator fin and evaluated its performance using 52,000 DWT bulker trials with/without stator fin. They also discuss the propeller rotation speed in an actual ship through voyage simulation.

Post-swirl devices. Research on post-swirl devices also has been carried out. This research includes:

Ryu et al. [2013] investigated the improvement of propulsive performance for ‘Turbo-Ring’, a Propeller Boss Cap Fin (PBCF)-like device to reduce the propeller hub vortex. Kawamura et al. [2013] showed the numerical result for PBCF performance in model and full

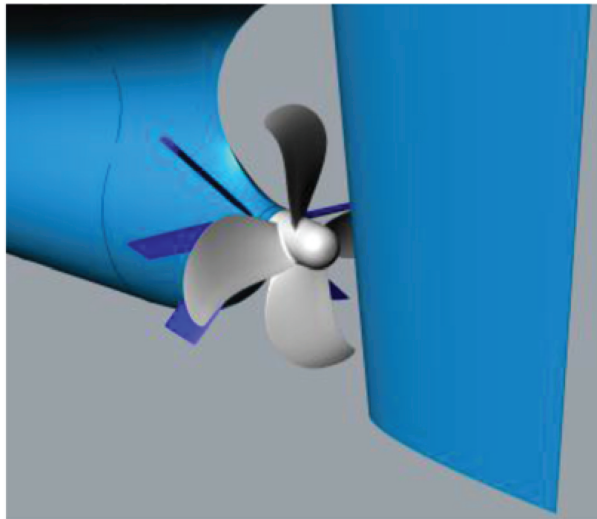


Figure 14 Example of a pre-swirl stator, Kim et al. [2014]

scales by CFD analysis. Two different types of propeller, conventional and highly skewed propeller, are used to investigate the effect of propeller type on the performance of PBCF. Lee et al. [2013] evaluated the propulsive performance of a rudder-fin equipped container ship. They simulated the performance using CFD under the conditions of both calm and seaway states. Druckenbrod et al. [2013] optimized PBCF to maximize propeller efficiency. They used an evolutionary optimization algorithm and obtain the optimal PBCF shape. Okazaki et al. [2015] investigated the performance of PBCF-like boss cap fin using CFD. They also showed the scale effect on the performance. Okada et al. [2015] developed a new rudder named “ultimate rudder” which is derived from a combination of propeller boss cap and rudder bulb.

Seo et al. [2016] precisely measured the flow behind PBCF using SPIV to clarify the effect of PBCF. Shon et al. [2016] applied the CAD automation algorithm and an optimization procedure to design an adapted twist rudder and demonstrated the design of a new rudder shape. Kim et al. [2016] studied comprehensive procedures from design to performance analysis for a cap fin including CFD, a model test, a sea trial and operation data analysis. From these data, they showed close to 2% energy savings

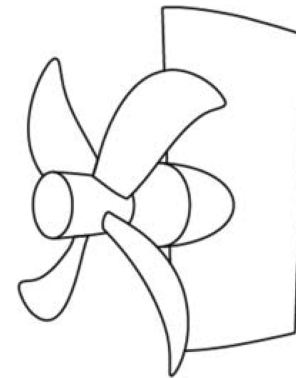


Figure 15 Concept of “Ultimate Rudder” proposed by Okada et al. [2015]

for a full scale boss cap fin.

Tandem propeller. Tandem propeller and contra-rotating propeller systems are also well-known methods to save energy. For instance, Igeta et al. [2013] developed a hybrid CRP system, which is the combination of an ordinary propeller and a ducted (Kort nozzle) propeller and showed the propulsive performance obtained from the experiment and CFD.

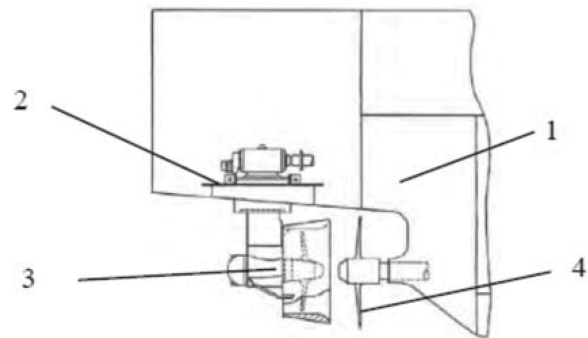


Figure 16 Schematic view of ducted tandem CRP, Igeta et al. [2013]

Sánchez-Caja et al. [2013] introduced TRIPOD project, one of EU projects in which a new concept of propulsion to improve the energy saving efficiency by use of the contra-rotating combination of POD propulsors and tip loaded endplate propellers. Model test and CFD results are presented. In addition, the scale effect for this system is discussed.

Propeller design. In the present report, we

placed “propeller design” here. Berger et al. [2013] showed a method to optimize a propeller by using the multi-objective method in the full-scale wake. In order to improve the propeller efficiency, Brown et al. [2014] studied the two types of tip load propellers to improve the propeller efficiency, and CFD simulations are carried out. Song et al. [2015] studied the hub-type and hubless rim driven thrusters (RDT) by use of CFD and demonstrated that higher efficiency is obtained with hubless RDT.

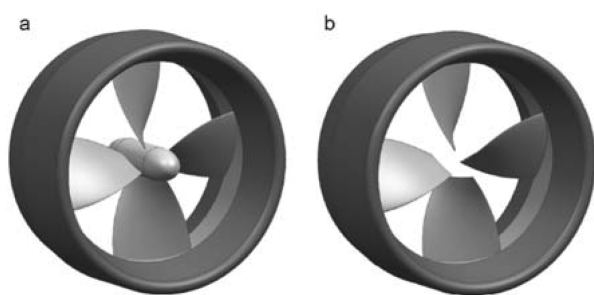


Fig. 1. A pair of hub-type and hubless RDT. (a) Hub-type RDT and (b) hubless RDT.

Figure 17 Hub-type RDT (left), Hubless RDT (right), Song et al. [2015]

Park et al. [2016] showed the design optimization method for a propeller considering the effect of ship hull and rudder effect by use of the vortex lattice method to evaluate propeller performance and CFD for evaluation of ship viscous flows. Ikeda et al. [2016] show a propeller design optimization method based on open source codes such as DAKOTA and Open FOAM. Van der Ploeg et al. [2016] applied a propeller with large diameter, hence the stern frame line formed a tunnel-like shape. Two different frame lines are designed to evaluate the propulsive performance with the large propeller.

A pod propulsor is one of the effective tools for energy saving propulsors and the estimation of its performance in full-scale is very important. Park et al. [2013] studied the performance of a podded propeller in full-scale by separately evaluating the propeller blade thrust and the pod casing drag. Shamsi et al. [2014] computed hydrodynamic forces acting on a pull/pusher type of podded propeller and

showed their propulsive performance.

#### 4.5 Operation

From the viewpoint of energy saving, ship operation is another important measure. For instance, weather routing is one of most well-known measures. Recently, in developing software to support navigation, researches in this category have been carried out widely at several organizations. For instance, Olsen [2013] discussed the e-NAVIGATION system, which helps ship operators to operate ships safely and optimally. Kano T. et al. [2014] studied a navigation system for domestic ship operation in Japan which can provide an energy-saving route and just-in-time speed plans. Kim et al. [2013] studied an optimal route finding problem for cruise ship design using the iterative dynamic programming and rhumb line formulation. Joint Operation for Ultra Low Emission Shipping (JOULES) worked an EU project introduced by Nagel [2014]. In the project, energy saving optimization is not focused on one design condition, but on real-life operation. Dinham-Peren [2015] studied trim and draft change as far as energy consumption is concerned. He also changed bow and stern profiles to investigate the effect of trim and draft on ship power. Altosole et al. [2016] investigated the effect of trim and draft changes on the ship resistance. Meanwhile, Sun et al. [2016] studied the trim optimization for a 4250-TEU container ship. Larsson et al. [2015] introduced a weather routing method based on a dividing rectangle (DIRECT) algorithm. From the viewpoint of actual ship operation, many works are presented in the RINA Conference EES 2015 (Energy Efficient Ships).

#### 4.6 Others

Some papers have presented a holistic review or investigation on energy saving methods. Van Terswiga [2013] considered the working principles of how the ESDs provide energy saving. He discusses three different type of ES-

Ds: pre-duct, pre/post swirl stators, rudder bulbs and their combinations. Minchev et al. [2013] presented a design of a 35,000DWT bulk carrier to meet EEDI requirements. In the design, hull-form design and propeller re-design, Mewis ducts are included. Hämäläinen et al. [2013] investigated an energy saving system for a twin or triple propeller cruiseliner. In the investigation, a holistic discussion is conducted on air lubrication, ducktail, bulbous bow, pod propulsor, hybrid CRP, pre-and post-swirl stator and design of the shaft line.

Monitoring of a full-scale ship gives important data to improve energy savings in ship operation. Newcastle University built a new catamaran research ship. One mission of this ship is full scale marine measurements and observation including wind farm and renewable device support, performance monitoring, and coating/fouling inspection. Adler et al. [2013] review the project.

#### 4.7 Effect on EEDI

EEDI has been enforced since 2013. The method of attaining EEDI is described in “2014 Guidelines on the method of the attained Energy Efficiency Design Index (EEDI) for new ships”, IMO MEPC. 1/Circ. 866. EEDI considers CO<sub>2</sub> emissions per capacity and  $V_{ref}$ .  $V_{ref}$  is ship speed in a calm sea condition on deep water.

Methods for survey and certification are described in “2014 Guidelines on survey and certification of the Energy Efficiency Design Index (EEDI)”, IMO MEPC.1/Circ.855/Rev.1.  $V_{ref}$  is preliminarily verified on model tests. Finally it is verified on the speed/power trials of the ship. For ships which cannot be conducted under the EEDI condition,  $V_{ref}$  is obtained from the conversion based on the model tests at the both drafts, trial condition and EEDI condition as shown in Figure 18.

$\alpha_p$  is the power ratio of power at trial con-

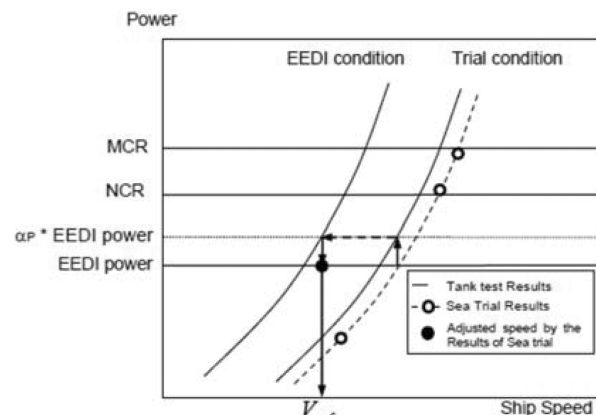


Figure 18 An example of scheme of conversion from trial condition to EEDI condition at EEDI power [MEPC.1/Circ.866]

dition predicted by the model tests and obtained by the speed power trials.

This is the important point of EEDI for ITTC and ESM committees. The power prediction for both drafts is essential for final EEDI verification.

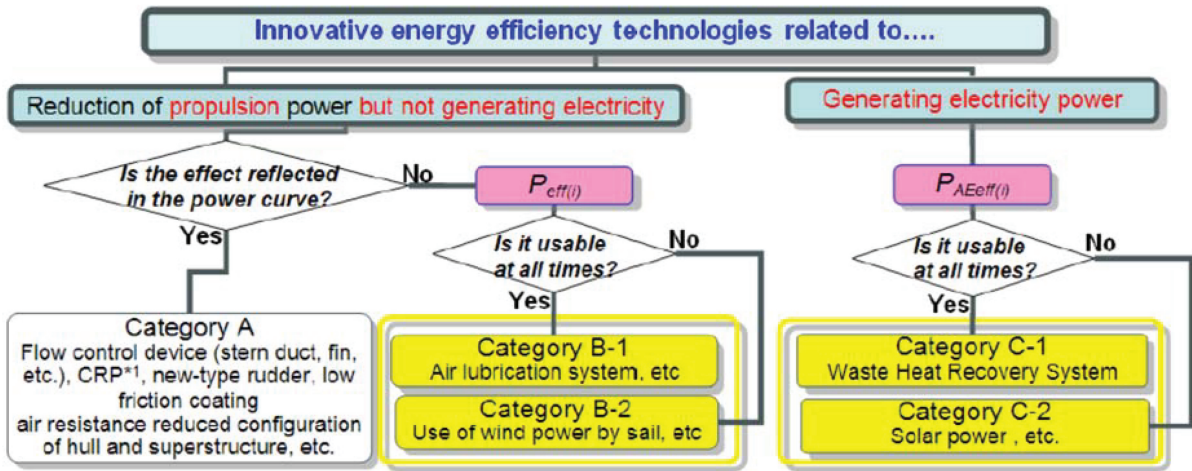
As for the energy saving method, the philosophy of IMO is written in the document MEPC 64/4/8, “Guidance on treatment of innovative energy efficiency technologies for calculation and verification of the attained EEDI.”

In the document innovative technologies are categorized as follows:

Category (A) : Technologies that shift the power curve, which results in the change of combination of  $P_p$  and  $V_{ref}$ : e.g. when  $V_{ref}$  is kept constant,  $P_p$  will be reduced and when  $P_p$  is kept constant,  $V_{ref}$  will be increased

Category (B): Technologies that reduce the propulsion power,  $P_p$ , at  $V_{ref}$ , but not generate electricity. The saved energy is counted as  $P_{eff}$ . Category (B-1): Technologies which can be used at any time during the operation and thus the availability factor ( $f_{eff}$ ) should be treated as 1.00.

Category (B-2): Technologies which can



\*1 Contra-Rotating Propeller

Figure 19 Innovative energy efficiency technologies [MEPC64/4/8]

be used at their full output only under limited condition. The setting of availability factor ( $f_{eff}$ ) should be less than 1.00.

Category (C): Technologies that generate electricity. The saved energy is counted as  $P_{AEff}$

Category (C-1): Technologies which can be used at any time during the operation and thus the availability factor ( $f_{eff}$ ) should be treated as 1.00.

Category (C-2): Technologies which can be used at their full output only under limited condition. The setting of availability factor ( $f_{eff}$ ) should be less than 1.00.

It is recommended that the above categorizations and treatment for  $V_{ref}$  should be adequate for all the energy saving methods. This is considered an important future effort.

## 5 USE OF WIND ENERGY

### 5.1 Wind Assisted Technologies

Wing sails. Lee et al. [2013] investigated the performance of multiple wing sails to

enhance ship thrust. They solve the flow around the wings using CFD to evaluate the generated thrust. Ouchi et al. [2013] introduced a new concept of wind sail ship "Wind challenger", in which the motor-assisted auxiliary system is applied. They carried out a voyage simulation and evaluate the energy saving rate of "Wind Challenger". Maria Viola et al. [2015] developed a velocity prediction program for ships with propulsion assisted by wing sails. The ratio between the propeller thrust of a ship with and without wings is used as a measure of the energy efficiency and showed the possibility to reduce the propeller thrust of a VLCC2 by up to 10% in cross winds. They concluded that the efficiency of the wing sails is crucial to achieving minimum savings with high aspect ratio wings performing best.



Figure 20 Image of "Wind Challenger" proposed in Ouchi et al. [2013]

Towing kites. Naaijen and Koster [2007] performed a theoretical analysis of potential fuel savings for a kite propulsion system. This included the effect of the propeller running in an off-design condition and concluded that the additional resistance due to leeway angle is small. Dadd et al. [2011] assessed different kite trajectories producing performance polar diagrams for a 300 m<sup>2</sup> kite. Different operation parameters are assessed such as aspect ratio and flight angle. Fagiano et al. [2012] investigated a high altitude kite system (200–600m) which is designed to generate electricity as the line is pulled as well as produce thrust. The Kite can then be winched in during a depowered condition producing a net energy production.

Flettner rotors. Pearson [2014] developed a model for assessing the performance gains from Flettner rotors and performed an initial assessment of the viability of retrofitting them to a specific ship. Craft et al. [2014] assessed Flettner-Thom rotors using RANS and LES with comparison to experimental data. They concluded that the Thom's multiple drums affected the boundary layer at low Reynolds numbers to improve the lift coefficients achieved.

## 5.2 In-Service Gains

Howett et al. [2015] developed performance prediction software that allows different wind assistance devices to be assessed. Modern square rigged sails (DynaRig), rotors and kites are assessed on one coastal and one ocean route. They concluded that sails and kites delivered between 9%–10% fuel savings whereas Flettner rotors provided 23%. Little difference was observed between the two routes however both had similar mean true wind speeds.

Traut et al. [2014] used numerical models of a Flettner rotor and a towing kite to assess their performance over five different trade routes concluding that different technologies

performed better on different routes. Bentin et al. [2016] assessed the optimal routing of a conventional multipurpose cargo ship with Flettner rotors operating in the north Atlantic and predicted energy saving between 20%–50% depending on ship speed and wind conditions.

Lloyds Register [2015] provides a review of wind assisted shipping, summarising quoted energy saving potential of different technologies and a cost analysis of payback periods for different fuel prices, fuels savings and capital investment required. They concluded that wind assistance is one of the few technologies that has the potential to provide double digit fuel savings. SOCP [2016] also provided a summary of wind assisted technologies concluded that a mean energy saving potential of 20% might be achievable.

## 6 CFD, EFD AND SCALING METHODS

### 6.1 CFD Methods for ESD

Compared with traditional model tests and theoretical research on ESD, the CFD method can decrease the design time and reduce costs significantly. Moreover, computer simulation will not affect the flow which may make the phenomenon of the flow become subtle.

Since 2010, most CFD research on ESD has been conducted to make the energy-saving mechanism clear and thereby pursue better structural designs. These included flow optimization devices, energy recovery devices, vortex reduction devices, new propellers and so on.

Many commercial software packages (e.g. FLUENT) and open software applications (e.g. OpenFOAM) are can be applied to ESD. In addition, many universities and institutions have developed their own codes to investigate ESD. For example, CMHL (Computational Marine

Hydrodynamics Lab) team led by Professor Decheng Wan at Shanghai Jiao Tong University has developed a CFD solver naoe-FOAM-SJTU based on OpenFOAM (Shen and Wan, 2014). As this solver implemented overset grid techniques, it can deal well with complex flow problems of ship-propeller-rudder multilevel and multi degree of freedom systems (Shen and Wan, 2014). Also, the resistance performance and manoeuver performance of ships can be solved with this package (Wang and Wan, 2016). Now, the naoe-FOAM-SJTU solver has been used in the study of the influence of ESDs on the propulsion performance of propellers.

Although great progress has been made in computer technology, attention is still required to mesh sensitivity and time step sensitivity in order to obtain a satisfactory result with rapid turnaround and low cost.

Model ship calculations with ESDs often require a refined mesh in the region where the ESD is mounted. Especially for a partially submerged propeller, the ventilation of blades needs to be captured accurately; hence there the mesh should be very fine. In order to guarantee computing efficiency and prediction accuracy, a mesh sensitivity test must be conducted with coarse, medium and finer grids. A  $\sqrt{2}$  is recommended as the ratio of law changing point number in three directions.

When it comes to time step sensitivity, two factors should be considered. On one hand, to retain convergence, the Courant number needs to be restricted to less than one, especially in multiphase flow. On the other hand, to retain accuracy in the simulation of the propeller, for normal ESD, the time step is usually determined by a propeller rotation of about two degrees. Additionally, it is strongly recommended that for a partially submerged propeller, the time step be equivalent to a propeller rotation of about 0.25 degrees.

To clarify the mechanism and the effec-

tiveness of the ESD, it is essential to investigate the propeller-rudder-ESD system. Methods based on potential flow theory and methods based on viscous fluid mechanics theory are both used in the numerical simulation of ESDs.

The potential flow theory including lifting-surface methods and panel methods is very mature and is applied widely in practical engineering. Keqiang Chen (2013) has done the design on the strut of a twin-screw ship based on the potential flow theory and the energy-saving effect of that was calculated. Cheng Ma (2014) investigated the integral optimization design of PBCF and the propeller. However, this method neglects the influence of the fluid viscosity and may result in numerical error which renders the calculation results valueless.

In recent years, the CFD method based on viscous fluid mechanics has developed rapidly along with great improvements in computer technology. This method includes viscosity and can better reflect the wake field of ESDs. Based on the theory, body force methods, sliding mesh methods, multi-reference frame methods and overset grid method have been developed and are widely used.

The body force method has a simple requirement of the ESD model and has high calculation efficiency. The source term of the body force can be obtained from the calculation of the propeller model based on the potential flow theory. Shaohua Wu (2013) investigated the working mechanism of Propeller Boss Cap Fins (PBCF) and found that PBCF could restrain the vortex.

A sliding mesh is usually used in the unsteady calculation and has a large computational load. While the sliding mesh is used, the computation domain is divided into two parts. One of them surrounds and rotates with the propeller, while the residual domain remains static. Grid numbers on both surfaces are not strictly required to be consistent, but the flux

must be equal, or the numerical computing process will become divergent. For example, He and Wan (2016) used the open software OpenFOAM to do the numerical simulation on the open water performance of the Contra-rotating propeller (CRPs) based on the sliding mesh. Yu Chang used the mixed surface comparison method and sliding grid to do the CFD numerical simulation on the CRPs. Wu and Wan (2016) compared the capability of the sliding mesh method and the dynamic overset grid by simulating a propeller with four blades.

Multi-reference frame method (MRF) is a kind of steady method. It has the advantage of a fast convergence speed, but has less accuracy than a sliding mesh. Andrea Califano and Sverre Steen (2009) used the MRF method to simulate the rotation of conventional propellers. Huibo Qi (2016) studied the energy-saving mechanism of the PBCF using MRF. Hailong Shen (2010) used the MRF method to study the scale effects of the rudder bulb and the rudder thrust fin. Haizhou Hu (2016) investigated the energy-saving effect of the thrust fin on a bulk carrier. Zhiqiang Rao (2012) used the sliding mesh technology to study the working mechanism of the pump jet propulsor.

The dynamic overset grid technology, including a hierarchy of objects that enable computation of control surfaces (rudders, stabilizers, ESD), opens the possibility of computation of complex motions (Shen and Wan, 2015). Yin, Wan, et al. (2015) conducted a numerical simulation on the JBC with the WED using the naoe-FOAM-SJTU solver which had the module of the overset grid based on the RANS equation. Sing-Kwan Lee (2012) studied the performance of a container ship with a thrust fin while its bow or stern was crashed with overset grid. Wenquan Wang et al. (2016), Sun, Wan, et al. (2016) also have applied the overset mesh to an ESD.

As the flow field of the ESD is usually complex, appropriate turbulence numerical sim-

ulation methods are needed. Generally speaking, Direct Numerical Simulation (DNS), Reynolds Average Navier-Stokes (RANS) and Large Eddy Simulation (LES) are the possible numerical techniques. DNS is seldom used for ESD simulation due to its required large computing power. RANS is the method used most often for the ESD calculations. For example, Fahri Celik (2007) used the commercial software, FLUENT to do the numerical simulation of the duct on a carrier. Based on RANS, the detailed wake field was computed. The paper focused on the analysis of the wake and the propulsion performance of the propeller while the carrier was at the speed of 10–16 knots. The results of the calculation showed that the WED could effectively improve the propulsion and reduce the viscous resistance if a ship had a large block coefficient. Also, it indicated that the installation of the WED had a great influence on energy-savings. Abdel-Maksoud (2003), Yin and Wan (2015), Shaofeng Huang (2012), Sun and Wan (2016), Hailong Shen (2016), Sunho Park (2014) and others also used RANS to conduct CFD simulation of ESDs.

LES uses a sub-grid model to simulate the effects of small-scale turbulence on large scale turbulence. Here the N-S (Navier-Stokes) equation is averaged or filtered to remove the small scale vortices from the flow field and the equation that satisfies large eddy is derived. Rickard E Bensow (2015) investigated the hull-propeller interaction of a single-screw transport ship at model scale using LES in both a baseline configuration and one with a pre-swirl stator installation. The analysis is focused on the unsteady effective wake, its impact on the propeller, and how this is affected by the installation of the stator blades upstream the propeller.

Comparing RANS and LES demonstrates that RANS is weak at simulating unsteady turbulence correctly and LES needs a large number of grids. To deal with the two drawbacks, DES (Detached Eddy Simulation) was put forward by Spalart and then developed to the so-

called DDES (Delayed Detached Eddy Simulation) model, which blends the standard Spalart-Allmaras RANS model and an LES model. In 2006, IDDES (Improved Delayed Detached Eddy Simulation) was put forward by Travin (2006) and Shur (2008) developed it into a mixed model of DDES and WMLES (Wall Modeled LES). Yin and Wan (2016) predicted resistance of full scale VLCC based on a S-A IDDES model.

Once the turbulence simulation method is decided, the specific turbulence model must be applied. Normally, realizable  $k-\varepsilon$  models are used in the simulation of ESD. The standard  $k-\varepsilon$  model is the simplest turbulence model for two equations. Xujian Lyu (2014) presented a mixture-model simulation of the two-phase microbubble flow over the hull of a SUBOFF model. The  $k-\varepsilon$  model has relatively better performance on the simulation of rotational flow. Hailong Shen (2016) studied the scale effect for a rudder bulb and a rudder thrust fin as regards propulsive efficiency.

The RNG  $k-\varepsilon$  model has better accuracy than the standard  $k-\varepsilon$  model and it can be used over an extensive range. Zhiqiang Rao et al. (2013) investigated the effect of the geometrical parameters on the pre-swirl stator using an RNG  $k-\varepsilon$  model. Tao Zhang (2011) investigated the unsteady performance of the contra-rotating propeller (CRP) based on an RNG  $k-\varepsilon$  turbulence model.

The so-called standard  $k-\omega$  model is a modification of the standard  $k-\varepsilon$  for the region of low turbulence strength. Skudarnov et al. (2006) tried to assess the role of mixture density variation in microbubble drag reduction based on a RNG  $k-\varepsilon$  turbulence model.

The SST  $k-\omega$  model is the most popular turbulence model, which can effectively blend the robust and accurate formulation of the standard  $k-\omega$  model in the near-wall region with the free-stream independence of the standard

$k-\varepsilon$  model in the far field (Menter, 1994). Naijun Lin (2014) analysed the influence of the designed circulation of the pre-swirl stator on the energy-savings. Takeo Nojiri et al. (2011) focused on the mechanism of Propeller Boss Cap Fins (PBCF) using a CFD method based on SST  $k-\omega$  turbulence model. Tao Sun, Decheng Wan (2016) evaluated the energy saving effect of a wake equalizing duct (WED) based on numerical results and experiment data, which were in good agreement using the SST  $k-\omega$  model. Yan Ma (2011), Yu Sun (2016), Lin Lu (2016) also applied the SST  $k-\omega$  model to investigate ESDs.

Besides the aforementioned issues, the scale effect is another point that should be investigated further. Until now, no recognized procedure for the investigation of the scale effect of ESD has been attacked. Some researchers attempted to study this issue. Hailong Shen (2016) focused on the scale effect of the rudder bulb and rudder thrust fin. Zhanzhi Wang (2016) tried to advance a new procedure on how to evaluate the scale effect of hybrid CRP pod propulsion system.

There are also some energy-saving methods that are different from the ESD mentioned above. Supercavity drag reduction, microbubble drag reduction, for example, are two kinds. Supercavity drag reduction tries to produce a gas cavity between the hull surface and the water which can reduce drag and improve navigational speed. Normally, the supercavity can be produced in three ways: increasing the speed of the ship; reducing the pressure of the flow field; ventilating the supercavity. Tianhong Xiong investigated the characteristics of the supercavitation drag reduction of a high-speed projectile with fins. S. Brizzolara et al. (2015) used CFD to study the performance of a new family of supercavitation hydrofoils. Mohsen Y. Mansour et al. did a comparative study of supercavitation phenomena on different projectiles shapes in transient flow. Yunfei Wu (2014), Xue Pao (2015), Daqiao Jin (2015),

Shiming Sun (2014), Yutian Li also have done some research on supercavity drag reduction.

Microbubble drag reduction works mainly through reducing the friction between the ship hull and the water. Qiongxia Xu (2013) investigated the drag reduction efficiency under different types of air nozzles, different speeds, different depths of draft and different nozzle forms. Lin Fang (2014), Yan Wei (2013), Huiping Fu (2016), Rui Li (2014), focused on microbubble drag reduction as well.

Based on the current status of research, future research on ESDs may focus more on the following aspects: (1) using CFD to optimize the ship profile and hydrodynamic ESDs at the same time; (2) using CFD to research the combination ESDs to obtain better design schemes; (3) conducting scale-effect research on ESDs; (4) research on bionic propulsion.

Suggestion: Along with the advancement of basic theories and computer technology, it is expected that CFD exhibit rapid development in the future. As there are all kinds of methods available for ESD, it needs a guideline which can better direct the research. A regulation is recommended to be established to play a helping role in the application of CFD on ESDs.

## 6.2 Experimental Methods for Energy Saving

Every testing facility for ESD performance assessment has its own test procedures and analysis method based on the ITTC 1978 performance prediction method. Since EEDI came into effect in Jan. 2013, experimental methods have remained the most reliable for the accurate estimation of ESD performance. However, the model tests are restricted to comparative study with/without ESD due to the lack of full-scale data and the absence of standard procedures. For instance, when testing facilities are required to conduct a test for a pre-swirl stator with duct (e.g. Becker Mewis Duct<sup>®</sup>), the dum-

my stern body and the ducted body are installed separately. Then the conventional resistance and propulsion tests are carried out with and without the ESD respectively. The analysis is made through the method described in the ITTC 22<sup>nd</sup> Unconventional Propulsors Committee report.

Well-known energy reduction mechanisms for improving the propulsion performance change the wake structure and reduce the loss of rotational energy by absorbing the propeller hub vortex. Hence the ship designers have tried to optimize ESD systems through the typical self-propulsion test. The pairs of fins attached to the hull, the duct with the fin, the pre-swirl stator and the rudder with bulb have been proven to be useful ESD systems when assessed through experiment. Lee et al. [2015] showed that the power savings by the reduction of hull resistance was correct with conventional model tests at design and ballast drafts in the SSMB (Samsung Ship Model Basin). To verify the performance of the SAVER Fin at full scale, sea trial tests were performed for a series of 35K bulk carriers.



Figure 21 A model ship equipped with SAVER Fin and SARB

Kim et al. [2016] studied the performance of the cap fin through CFD, model testing, sea trials and operational data analysis. However it is difficult to achieve accurate assessment of the actual power savings due to scale effects. As generally reported, the cap fin showed better power savings effect at full scale than model scale. Even though the operational data are

insufficient for reliable analysis, the cap fin effect in power savings might be roughly 2% at full scale as realized in a sea trial.



Figure 22 Absorption of hub vortex with DSME cap fin

As the ESD after the propeller, there are rudder systems. Sasaki et al. [2016] developed In addition to the propeller, there are rudder systems for ESD. Sasaki et al. [2016] developed a new twin rudder system ‘gate rudder’ with asymmetric wing section, aside a propeller. The gate rudder system shown in Figure 23 is expected to provide the duct effect, so that energy savings of 7%–8% was anticipated potentially.



Figure 23 Aft view of a ‘gate rudder’

To reduce the added resistance in waves, many attempts for new conceptual bow shapes have been made. Sakurada et al. [2016] has developed a new ship bow shape named COVE (see Figure 24). In tank tests, the performance of the COVE bow has been confirmed by the frequency response of added resistance and

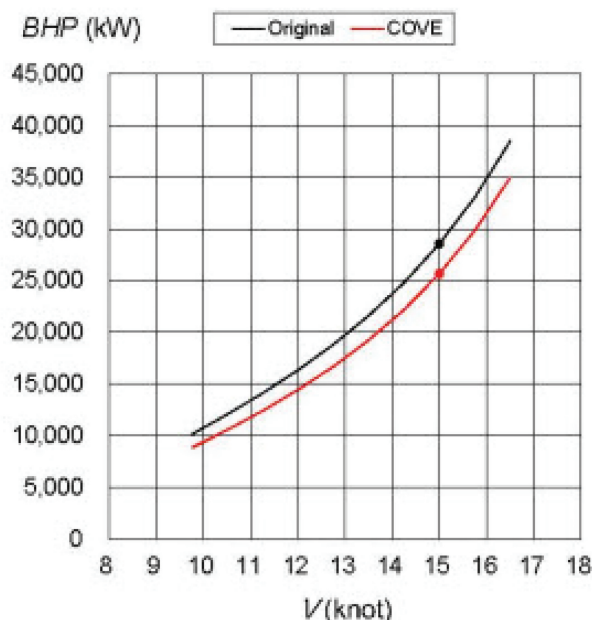


Figure 24 The relationship of the ship speed and the brake power in BF6 of head wind and waves

ship motion in head and beam waves. As a result, it is clarified that the COVE bow reduces the added resistance in waves about 40% in head waves compared with the original bow. From figure 24, it is found that COVE can reduce BHP about 10% at BF6 of head wind and waves at 15 knots.

Lee et al. [2016], evaluated the added resistance of a new Hi-Bow applied to the VL-CC, through a series of model tests in the deep water towing tank of HMRI (Hyundai Maritime Research Institute). The model ship was free to surge, heave, roll and pitch. The lay-out of the model set-up is shown in the figure 25. In the full load condition, the added resistance was reduced by about 40% for the Hi-Bow.

Oh et al. [2017] have studied the experimental techniques for added resistance in waves, which were free running, soft mooring and the conventional captive test. An LNG Carrier was chosen and tested with those three tests at the SSMB. The test condition was at the design draft, and head seas with regular waves,  $\lambda/L$ : 0.3–2.0 at 13.0, 19.5 knots.

Recently one of the most frequent tank

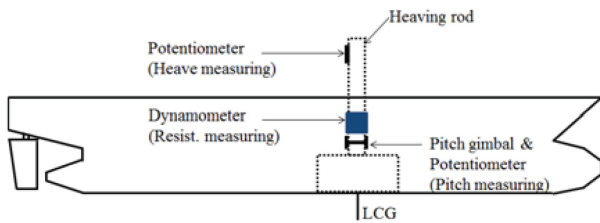


Figure 25 Model set-up for measurement of Hi-Bow

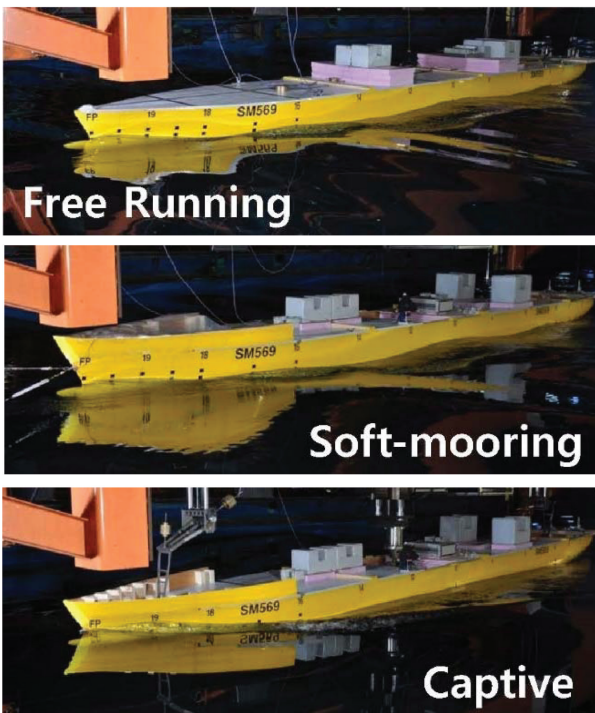


Figure 26 Free running, Soft-mooring, Captive set-up for the measurement of the added resistance in waves

tests for energy savings is to seek the optimum initial trim. Most ship owners require their ships to be operated under the optimum trimmed attitude. However they prefer digital simulation to the model test because those series of test are not cost and time effective. Moreover, when the ship has ESDs such as ducts or fin, each testing facility has their own test procedure and analysis methods. These need to be identified and hence it is necessary to make a model test procedure for the trim optimization test with ESDs.

### 6.3 Scaling Methods for ESD

Many hydrodynamic energy saving devices have been designed, optimised and tested at model scale and yet these questions remain for ship operators: How do these devices perform at full scale and are these energy savings achievable in sea trials and under actual operating conditions?

Although the ITTC Performance Prediction Method (7.5-02-03-01.4) recommends the best practice for considering scale effects it, relies on results from Resistance tests and Self-propulsion tests. The Propulsion test procedure recommends that the duct of a ducted propeller should be included in the open water test and also that the resistance generated by appendages must be scaled using three methods. However, there are challenges that make hydrodynamic behaviour of ESDs inherently different at the two scales.

Firstly, Reynolds numbers are much higher at full scale and the boundary layers are not scaled-up with the scale factor. An ESD at model scale may be located inside the boundary layer due to relatively low Reynolds number whereas at full scale the boundary layer is thinner with respect to ship length and the ESD will be partially located inside boundary layer. The wake fraction will be smaller and thus the ESD behaviour will differ.

Secondly, the flow separation at full scale is delayed and vortices from bilge keels and appendages are weaker or diminish before the propeller plane, and therefore the flow pattern at the propeller plane will differ from that at model scale.

Moreover, it is not clear what value should be used for the Skin Friction Correction Factor for a hull fitted with an ESD; some have used a constant value in the self-propulsion test for both the bare hull and the appended hull

with ESD. The other challenge is that Pre-swirl devices such as wake equalising ducts and fins cannot be easily included in open water tests. On the other hand, post-swirl devices such as the twisted rudder influence the propeller performance and cannot be considered as an appendage only in resistance tests, and yet it is not clear how they should be considered in the open water test.

Thus, many studies have tried to evaluate the scale effect on various ESDs. Hansen et al. (2011) and Kawamura et al. (2012) believed ESDs are more effective at full scale compared to what is observed/measured in a test basin.

As full scale data are either not available for many designs or are not very accessible, some researchers have used CFD techniques for the two scales. Hai-Long et al. (2016) evaluated the impact of a rudder bulb and a rudder thrust fin on propulsive efficiency in a self-propulsion test using the MRF technique for propeller modelling. Bhattacharyya et al. (2016) investigated the scale effect on open water characteristics of a controllable pitch propeller working within different duct designs. In contrast, Zhao et al. (2015) studied effects of a duct in a self-propulsion test at two scales. Park et al. (2015) assessed a pre-swirl stator fin in a self-propulsion test at two scales by using the sliding mesh technique in the propeller modelling. Park et al. (2014) carried out a numerical analysis on turbulent flow around a pre-swirl stator fin at model and ship scale. Similarly, Si et al. (2014) investigated the scale effect on hull-ducted propeller interaction. There are also some numerical studies on scale effect on form factor (e.g. Kouh et al. 2009; Raven et al. 2008). Park (2015) investigated the scale effects on flat plate friction resistance and proposed a new friction line for flat plates. In a numerical resistance test at two scales, Guo et al. (2015) attempted to propose a non-geometrically similar model for predicting the wake field at ship scale. Lin et al. (2015) carried out a numerical study on scale effects on thrust de-

duction in self-propulsion procedure. Choi et al. (2015) assessed the scale effect on performance of a tractor type podded propeller.

There are also some studies that compared the tank test results with sea trials and evaluated the scale effect. A recent FP7 project GRIP (Green retrofitting through optimisation of hull-propulsion interaction) investigated a few ESDs. Prins et al. (2016) reported that pre-swirl stator fins design was superior and then it was installed on a vessel. The vessel performance was measured before and after fins installation. Zuo et al. (2015) carried out a sea trial validation on energy saving effects of a wake improving duct combined with propeller boss cap fins. Lee et al. (2015) compared fins effectiveness in the tank test with that of a sea trial. Kim et al. (2013) optimised a pre-swirl stator design in CFD and then tested it in the tank and measured their performance at sea. Similarly Hooijman et al. (2010) compared the performance of pre-swirl stator fins in a tank with that at sea. An early study in 1991 by Okamoto et al. designed a rudder fin in the tank and observed good agreement with the subsequent sea trial. A recent study by Kumagai et al. (2015) deployed a theoretical approach to evaluate performance of a hydrofoil in air bubbles to reduce ship drag. He then tested it in a self-propelled experiment and finally measured its impact on ship operation.

## 7 FULL SCALE DATA

### 7.1 Background

Very little full scale data have been found, this in light of the fact that full scale measurement is not easy. It requires special skill to obtain quality measurements. In addition, for merchant ships it is difficult to get time to conduct measurements.

Additionally we have to consider the intel-

lectual property issue. The hull form data and energy saving devices are also necessary for CFD studies. However, the data have not been made available by the owners.

One of the aims of full scale data for ESM is to compare the ESD/ESM effects in actual ships to model tests. The mechanism is not always the same between model and full scale.

While CFD researchers are attempting to solve this, data for validation are scarce.

## 7.2 Survey of Literature

Table 3 shows the full scale data found by a survey of the literature. The number of papers is very small.

**Table 3 List of full scale data**

ESM	Ship type	Full scale data	Gain	Reference
Hub fin	Tanker	Sea trial	3.5-3.8%	Hans Richard Hansen et al. (2011)
Hub fin	Car ferry	Operation data	2.8%	Kenta Katayama et al. (2015)
Hub fin	Gas carrier	Sea trial (Operation data)	1.5-2.0%	Woojin Kim et al. (2016)
Fin, rudder bulb	Bulk carrier	Sea trial	7.4%	Hee Dong Lee et al. (2015)
Pre-swirl stator	Bulk carrier	Sea trial	7%	Yan Xing-Kaeding et al. (2015)
Air lubrication	Tanker	Sea trial	3.8,4.3%	Noah Silberschmidt et al. (2015)
-	ConRo-ship	PIV	-	Andre Kleinwächter et al. (2015)

Hub fin. Some papers were found on the hub fin. This is because the hub fin is one of the easiest energy saving devices. It can be installed as retrofit. Teekay Corporation installed a PBCF to an Aframax tanker at the quay over a three days period, see Figure 27, Hansen et al. (2011). They confirmed the effects of a PBCF by a sea trial before and after fitting of the PBCF. About 4.0% power savings was confirmed.

Nakashima Propeller Co., Ltd. verified their hub fin, ECO-Cap by installing to a Car ferry in service shown in Figure 28, Okazaki et al., 2015. The FOC was monitored before and after ECO-Cap installation and was confirmed 2.8% decrease in average.

Kim et al. evaluated DSME Cap Fin for LNGC by sea trial and operation data. The speed was improved 0.1knot at the sea trial and much more based on operation data.

Other ESD. Samusung Heavy Industries developed the SAVER Fin which is a simple fin-shaped appendage attached at the stern bilge area, Figure 29. To verify the performance of the SAVER Fin at full scale, sea trial tests were performed for two bulk carriers, with and without SAVER Fin, Lee et al., 2015. The result of sea trial showed 7.4% power saving by the SAVER fin.

HSVA has performed the hydrodynamic design of a Pre-Swirl Stator for a bulk carrier. Extensive sea trials of this ship without and



Figure 27 Fitting the PBCF, Hansen et al., 2011



Figure 28 ECO-Cap attached actual ship



Figure 29 SAVER FIN, Lee et al., 2015

with a stator were performed in short sequence. The trial results saw a reduction of nearly 7%

power at equal speed, Xing-Kaeding et al., 2015.

The Silverstream System which is an air lubrication technology was installed on a 40,000 DWT product carrier. The net power saving of the trial was calculated to be 3.8% on the laden condition. It was 4.3% on the ballast condition. Silvershmidt et al., RINA ESS 2015.

Detail data in full scale. In the papers above only power savings have been discussed. More detailed data, such as velocity or pressure distribution, are required to investigate the mechanics, scale effect and to verify CFD results.

Univ. of Rostok, Kleinwächter et al. (2015) carried out PIV measurements for cavitation research at Con-ro ship by major conversion to measure, see Figures 30 and Figure 31. It is requested that similar measurements be made for ESMs.

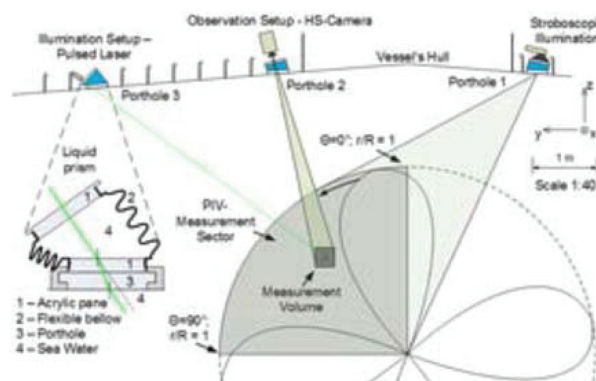


Figure 30 Measurement principal, Kleinwächter et al., 2015

Hull and ESD data. For the validation of CFD, not only the detailed hydrodynamic data is required at full scale but also the hull and ESD data are required.

Lloyd's Register held a 2016 Workshop on Ship Scale Hydrodynamic Computer Simulation. The target ship was the General Cargo built in 1994. The hull data was measured by 3D scan and distributed to participants, Figure



Figure 31 PIV Measurement setup in the steering gear compartment, Kleinwächter et al., 2015

32. Through comparisons of blind simulation results submitted by participants, and the comprehensive ship trials carried out by LR, the workshop demonstrated that ship speed could be predicted within approximately 4% of actual trial speeds.



Figure 32 3D laser scanning in a dry-dock, Lloyd's Register, 2016

Conclusion. We need more full scale data, not only power saving data, but also detailed data such as velocity and/or pressure distributions as changed by ESMs. In order to obtain detailed data, a comprehensive research project might be effective. The intellectual property issue also needs to be solved.

## 8 NEED FOR NEW PROCEDURES

There is a real lack of procedures and guidelines for ESD. This is a challenge going forward given the different nature of potential methods and devices. Furthermore full scale validation data are required to verify such guidelines, which currently do not exist. Additional collaboration with the PC will be required to make progress in this area in the future.

Referring to the table of methods, it is suggested that guidelines or procedures are required for all of these to standardise assessments in the future. Some examples of how this could be done are provided below.

### 8.1 Guideline on Skin Friction Scaling

The 28<sup>th</sup> ITTC has decided to publish a new guideline titled “Resistance Test and Performance Prediction Method with Skin Frictional Drag Reduction Techniques”. The purpose of the procedure is to complement the existing procedures for the resistance and propulsion model tests when skin frictional drag reduction techniques are employed in the model test to predict the full scale performance. Such techniques include air lubrication, low frictional coating and hull appendages. The existing resistance and propulsion performance prediction method are not applicable in such cases, because the model-ship extrapolation is based on the skin frictional drag coefficient for the “baseline” surface without skin frictional drag reduction.

Skin frictional drag reduction has been noted as an effective way to improve the fuel efficiency of ships. This is because the skin frictional drag is the major resistance component, occupying more than 60% of total resistance for Froude numbers below 0.15. The most noticeable technique is air lubrication, where

air is injected onto the hull surface to form a bubbly flow or air layer (Jang et al. 2014). Application of low frictional anti-fouling coating (Yang et al. 2014) could be an alternative way to achieve skin frictional drag reduction. Yet another possibility is the surface mounted hull appendage like outer-layer vertical blades array (An et al., 2014). Although these techniques vary in the underlying physical mechanism leading to skin friction reduction and the quantitative drag reduction efficiency, they pose a significant common issue performance prediction based on the scaled model test. The extrapolation method in the existing performance prediction procedure is based on the ITTC 57 Model-Ship Correlation Line originated from the ATTC line

$$0.242/\sqrt{C_F} = \log_{10}(\text{Re} \cdot C_F),$$

which is an empirical skin friction correlation for a smooth surface. Therefore, if a certain skin frictional drag reduction technique is employed in a model test, then the skin frictional characteristics of the model will no longer follow the existing Model-Ship Correlation Line, leading to an incorrect performance prediction of the full-scale ship. This draft guideline proposes a new scaling method which can be employed when a skin frictional drag reduction technique is employed in a model test.

Depending on the nature of the skin friction techniques, different extrapolation methods need to be employed. In the present guideline, the skin friction techniques are to be divided into two categories: homogeneous and inhomogeneous.

In the homogeneous category, the entire surface characteristics are modified so that the skin frictional drag reduction occurs everywhere. Low frictional coating falls in this category. In this category, the presence of a drag reduction mechanism at a particular location is scarcely affected by the local conditions such as pressure gradient, surface curvature, etc. In

addition, the skin friction reduction effect can hardly be switchable, so the comparison between model tests with skin friction reduction (hereinafter called an “SFR” test) and without skin friction reduction (hereinafter called a “BASELINE” test) would require two identical models. This is however, impractical in most cases, so the comparison between two states needs to be performed in a canonical flow around simpler geometry, i.e., a total drag measurement of a towed flat plate or a floating-element skin friction measurement in a turbulent boundary layer developing in a circulating water tunnel. The advantage of a canonical test is that the “BASELINE” test result as well as the “SFR” test result can be compared with an empirical correlation such as the ATTC line

$$0.242/\sqrt{C_F} = \log_{10}(\text{Re} \cdot C_F)$$

for a smooth surface.

In the inhomogeneous category, the boundary layer is influenced locally and the skin friction effect takes place at certain locations. Air lubrication, polymer injection and replaceable hull appendages belong to this category. Taking air lubrication for example, the local skin friction greatly varies whether the injected air layer is present or not in the immediate vicinity of the location in question. As the drag reduction mechanism (presence of injected air/polymer, interaction between appendage and boundary layer) is strongly affected by the local conditions, the drag reduction effect cannot be quantified in terms of canonical flow measurement. Also the skin friction reduction effect can be turned “ON” and “OFF” in this category. Therefore, a single model would suffice for both the SFR test and the BASELINE test. In this draft guideline, attention is paid to set up a procedure to carry out model test and then to extrapolate to full scale for the inhomogeneous techniques.

## 8.2 Proposing a Future Guideline on the Scaling Method for Pre-Dwirl Devices

The powering performance prediction method for the model test of a conventional ship has been established by ITTC in 1978. The ITTC 1978 method has been successfully applied to single screw conventional ships. With a view to reducing EEDI of marine vessels, various kinds of ESD (Energy Saving Device) have been devised to improve hull form and propulsion system. Typical ESDs are PSS (Pre-Swirl Stator), PSD (Pre-Swirl Duct), CRP (Contra Rotating Propeller), PBCF (Propeller Boss Cap Fin), etc.

PSS, which is located in front of the propeller, improves the propulsion efficiency through the recovery of rotational energy generated during propeller rotation, making a counter-swirl flow against the tangential velocity caused by the propeller. The device achieves about 5% reduction in energy consumption (Lee et al., 1994; Kim et al., 2004). PSD, which also is located in front of the propeller, consists of two ESD: PSS and duct. The device makes the oncoming flow more uniform to the propeller. Although the performance varies according to ship type and operating condition, its energy reduction effect is about 3% to 6% (Mewis and Guiard, 2011; Dang, 2012; Shin et al., 2013; Song et al., 2015).

Recently, Lee (2015) carried out a comparative full-scale performance prediction for the pre-swirl devices based on the ITTC1978 method and the ITTC1999 method. It was stated that the ITTC 1978 method has a limitation for extrapolating for such a pre-swirl device. The ITTC 1999, a newer procedure which adopts different scaling for the axial and tangential component of wake, did not appear to clarify the flow mechanism around the propeller section. It was then proposed a new extrapolation method which leads to a more reasonable estimate for the angle of attack to the propeller. This approach will be presented by Kim et al.

(2017) at the 5<sup>th</sup> International Symposium on Marine Propulsion and the corresponding extrapolation formula is given as follows:

$$w_{ss} = (t_{MS} + 0.04) + (w_{MS,Axial} + t_{MS} - 0.04) \frac{C_{FS} + C_A}{C_{FM}} + w_{MS,Tangential} \quad (1)$$

$$w_{MS,Axial} = w_{MO} + (w_{MS} - w_{MO}) \cdot \text{Factor}_{Axial} \quad (2)$$

$$w_{MS,Tangential} = (w_{MS} - w_{MO}) \cdot \text{Factor}_{Tangential} \quad (3)$$

where  $w_{ss}$  = effective wake with pre-swirl device at full scale;  $w_{MS}$  = effective wake with pre-swirl device at model scale;  $w_{MO}$  = effective wake without pre-swirl device at model scale; and  $t_{MS}$  = thrust deduction with pre-swirl device at model scale.

In these formulae, the thrust deduction factor is changed from that without a pre-swirl device in the ITTC 1999 method to that with a pre-swirl device. It was found that the portions of tangential and axial velocity varies according to the vessel type as well as the device type. As shown in Table 4, Kim et al. (2017) proposed the factors of axial and tangential portion to be 0.3 and 0.7 in PSS case and 0.8 and 0.2 in PSD case, respectively.

**Table 4 Factors of axial and tangential portion**

ESD Type	Factor <sub>Axial</sub>	Factor <sub>Tangential</sub>
PSS	0.3	0.7
PSD	0.8	0.2

The newly proposed method is then applied to extrapolate model test results for KCS and KVLCC in comparison with ITTC 1978 and ITTC 1999 methods. Whilst the three methods give almost the same values for the thrust deduction factor, the new method (Kim et al. 2017) gives the values of the full scale wake, delivered power and speed of revolution to lie between the values given by the ITTC 1978 and ITTC 1999 methods. In case of PSS, the new method gives estimates closer to those by ITTC 1999. On the other hand, the esti-

mated values by the new method for PSD are closer to those by ITTC 1978. As the newly proposed method is based on CFD simulation results, it needs to be verified by results obtained using such detailed flow measurement techniques as LDV and PIV. Furthermore, feedback from more comprehensive full-scale data will be required to establish and refine the extrapolation strategies proposed.

## 9 CONCLUSIONS

A brief summary of each of the substantive sections of this report is presented highlighting them. Additionally potential tasks for the next committee are provided.

In section 3, a thorough discussion of techniques to reduce skin-friction drag is presented. Conclusions are organized according to sub-section headings. As regards passive methods, it seems that super-hydrophobic surfaces offer the most friction drag reduction, but issues such as biofouling are largely unknown/unresolved for use of these surfaces on ships. Additionally surface coatings have seen laboratory success. Active methods abound with polymer injection successful but too expensive (except perhaps for military use), bubble injection lacks downstream persistence, and partial-cavity drag reduction has associated control issues; hence air layer drag reduction remains the most logical proven method. Other active methods (heating/cooling, electromotive, blowing and suction, wall motion) have been successful in the lab, but are largely not cost effective. A discussion of roughness both random and patterned is given as is a brief discussion of biofouling and attempts to mitigate it, which have had limited success.

Section 4 categorises and discusses the ESMs available at the time of this publication. Furthermore, it provides references from the recent literature of the 22 ESMs and then discusses each of them in turn. It provides back-

ground for the subsequent sections as well as a general review of each of the energy saving methods.

In section 5 the recent literature on wind-assisted propulsion is assessed. This remains one of the few possibilities for realising double digit energy savings for commercial ships however issues associated with capital cost, crewing requirements and unpredictability of weather conditions remain as challenges to uptake.

Section 6 is an in-depth discussion of computational fluid dynamics, experimental fluid dynamics, and scaling methods as each relates to energy saving methods and devices. In section 6.2, the new or specially proposed experimental methods or test schemes for ESD were shown to be largely absent since 2013, and studies on verifying and validating ESD performance through model tests have been shown to be lacking also. Additionally it is necessary to identify the optimum initial trim and to make an appropriate test procedure for ESDs.

Full scale data were to be the subject of section 7; however these datasets were found to be severely deficient. It was concluded that we need more full scale data, not only power saving data, but also detailed data such as velocity and/or pressure distributions as changed by ESMs. To obtain detailed data, a comprehensive research project might be effective. The intellectual property issue also needs to be solved.

Section 8 presents a new guideline on skin friction scaling. Furthermore it provides a path to a future guideline for pre-swirl devices.

### 9.1 Potential Tasks for the Next Committee

(1) Continue a systematic survey of energy saving methods (excluding machinery), devices, applications and possible savings, including the influence on the EEDI formula. Identifi-

fy the effect of energy saving methods on different sea trial and EEDI drafts. Consider a complementary metric to EEDI to represent power savings.

(2) Continue identifying and updating the physical mechanisms for the newly introduced energy saving methods.

(3) Update a survey on frictional drag reduction methods, including air lubrication and surface treatment.

(4) Update a survey on energy savings based on the use of wind energy.

(5) Continue to monitor the CFD methods, model tests and scaling for energy saving devices. Take into account Tokyo 2015 CFD workshop results investigating the influence of ESD.

(6) Continue to identify the needs for new model test procedures (resistance and propulsion, extrapolation methods) to investigate the effect of energy saving methods.

(7) Collect full scale data obtained through relevant benchmark tests on the effect of energy saving methods. Use the full scale data for validating the effect of ESM. Develop a guideline to conduct in-service performance evaluation for ESM.

(8) Identify and recommend the tasks related to energy saving methods and devices that should be undertaken during the 30th ITTC by standing committees.

## 9.2 Recommendations to the Conference

The 28th ITTC Specialist Committee on Energy Saving Methods recommends adopting the new guideline on ‘Resistance Test and Performance Prediction Method with Skin Frictional Drag Reduction Techniques’.

## 10 REFERENCES

- Abdel -Maksoud, M., 2003. “ Numerical and experimental studyof cavitation behaviour of a propeller. Sprechttag Kavitation, Hamburg” [https://www. researchgate. net/ publication/ 237269234\\_Numerical\\_and\\_Experimental\\_Study\\_of\\_Cavitation\\_Behaviour\\_of\\_a\\_Propeller](https://www.researchgate.net/publication/237269234_Numerical_and_Experimental_Study_of_Cavitation_Behaviour_of_a_Propeller).
- ABS, 2015. Ship Energy Efficiency Measures: Status and Guidance (2015) accessed from [https://www. eagle. org/eagleExternalPortal-WEB/ShowProperty/BEA% 20Repository/References/Capability% 20Brochures/ShipEnergyEfficiency](https://www.eagle.org/eagleExternalPortal-WEB/ShowProperty/BEA%20Repository/References/Capability%20Brochures/ShipEnergyEfficiency).
- Agostini, L. Toubert, E. and Leschziner, M.A., 2014, “Spanwise oscillatory wall motion in channel flow: drag-reduction mechanisms inferred from DNS-predicted phase-wise property variation at  $Re_{\tau} = 1000$ ,” Journal of Fluid Mechanics, vol. 743, 606-635
- Agrusta .A., Bruzzone D., “Study And Experiments On the Hull Resistance Reduction By Air Ventilation In Calm Water For Semi-Displacement Hulls” NAV 2015 (2015) pp.208-218
- Alame, K. and Mahesh, K., 2015, “Direct Numerical Simulation of Superhydrophobic Surfaces,” APS Div. Fluid Dyn. Annual Meeting
- Altosole M., Figari M., Ferrari A., Bruzzone D., Vernengo G., “Experimental and Numerical Investigation of Draght and Trim Effects on the Energy Efficiency of a Displacement Mono-Hull” ISOPE 2016 (2016) Vol.4 pp. 857-863
- Amromin, E. and Mizine, I., 2003, “ Partial cavitation as drag reduction technique and problem of active flow control,” Marine

- Technology, vol. 40, no. 3, pp. 181-188.
- An, N. H., Ryu, S. H., Chun, H. H. and Lee, I., 2014, "An experimental assessment of resistance reduction and wake modification of a KVLCC model by using outer-layer vertical blades," International Journal of Naval Architecture and Ocean Engineering, vol. 6, no. 1, pp.151-161
- Andrea Califano, Sverre Steen. "Analysis of different propeller ventilation mechanisms by means of RANS simulations". First International Symposium on Marine Propulsors smp' 09, Trondheim, Norway, June 2009.
- Andrewartha, J., 2010, "The effect of freshwater biofilms on turbulent boundary layers and the implications for hydroelectric canals," Ph.D. Thesis, University of Tasmania
- Antonia, R. A., Zhu, Y., and Sokolov, M., 1995, "Effect of Concentrated Wall Suction on a Turbulent Boundary Layer," Physics of Fluids, vol. 7, no. 10, pp. 2465-2474.
- Atlar M., Aktas B., Sampson R., Seo K-C., Viola I. M., Fitzsimmons P., Fetherstonhaugh C., "A Multi-Purpose Marine Science & Technology Research Vessel For Full-Scale Observations And Measurements" AMT' 13 (2013)
- Atlar M., Bashir M., Turkmen S., Yeginbayeva I., Carchen A., Politis G., "Design, Manufacture And Operation of A Strut System Deployed on A Research Catamaran to Collect Samples of Dynamically Grown Biofilms In-Service" AMT' 15 (2015)
- Åvist P., Pyörre J., "Modeling the Impact of Significant Wave Height and Wave Vector using an On-board Attitude Sensor Network", *compit' 13* (2013), pp.293-300
- Bandyopadhyay, P. R., Henoeh, C., Hrubes, J. D., Semenov, B. N., Amirov, A. I., Kulik, V. M., Malyuga, A. G., Choi, K.-S. and Escudier, M. P., 2005, "Experiments on the effects of aging on compliant coating drag reduction," Physics of Fluids, vol. 17, 085104 (9 pages).
- Baron, A., and Quadrio, M., 1996, "Turbulent drag reduction by spanwise wall oscillations," App. Sci. Res., vol. 55, pp. 311-326.
- Bensow R., "Large Eddy Simulation of a Cavitating Propeller Operating in Behind Conditions with and without Pre-Swirl Stators", *smp' 15* (2015) pp.458-477
- Bentin, M., Zastrau, D., Schlaak, M., Freye, D., Elsner, R. and Kotzur, S., 2016. "A new routing optimization tool-influence of wind and waves on fuel consumption of ships with and without wind assisted ship propulsion systems." Transportation Research Procedia, 14, pp.153-162.
- Berger S., Druckenbrod M., Pergande M., Abdel-Maksoud M., "Testing a Semi-Automated Tool for the Optimisation of Full-Scale Marine Propellers Working behind a Ship" MARINE 2013 (2013) pp.512-529
- Berger, T. W., Kim, J., Lee, C. and Lim, J., 2000, "Turbulent boundary layer control utilizing the Lorentz force," Physics of Fluids, vol. 12, no. 3, pp. 631-649.
- Berman, N.S., 1978 "Drag reduction by polymers," Annual Review of Fluid Mechanics, vol. 10, pp. 47-64.
- Bertram V., Hochkirch K., "Optimization for Ship Hulls-Design, Refit and Operation." MARINE 2015 (2015) pp.210-217
- Bewley, T. R. and Aamo, O. L., 2014, "A 'win-win' mechanism for low-drag transients in controlled two-dimensional channel flow and its implications for sustained drag reduction," Journal of Fluid Mechanics, vol. 499, pp. 183-196

- Bhaganagar, K., Kim, J. and Coleman, G., 2004, "Effect of Roughness on Wall-Bounded Turbulence," *Flow, Turbulence and Combustion*, vol. 72 (2), 463-492
- Bhattacharyya A., Krasilnikov V., Steen S., "Scale Effects on a 4-Bladed Propeller Operating in Ducts of Different Design in Open Water" *smp' 15* (2015) pp.587-594
- Brenner M., Harries S., Kroger J., Rung T., "Parametric-adjoint Approach for the Efficient Optimization of Flow-Exposed Geometries" *MARINE 2015* (2015) pp.230-241
- Brenner M., Zagkas V., Harries S., Stein T., "Optimization Using Viscous Flow Computations for Retrofitting Ships in Operation" *MARINE 2013* (2013) pp.69-80
- Brizzolara S., Bonfiglio L., "Comparative CFD Investigation on the Performance of a New Family of Super-Cavitating Hydrofoils", 9th International Symposium on Cavitation (CAV2015), Vol. 656, no. 1, pp. 144-147.
- Brown M., Sánchez-Caja A., Adalid J. G., Black S., Pérez Sobrino M., Duerr P., Schroeder S., Saisto I., "Improving Propeller Efficiency Through Tip Loading" 30th SNH (2014)
- Bugalski T., Szantyr J.A., "Numerical Analysis of Propeller-induced Pressure Pulses in Wakes Modified by Improvement Devices" *NuTTS 2014* (2014)
- Butterworth J., Atlar M., Shi W., "Experimental Analysis of an Air Cavity Concept Applied on a Ship Hull to Improve the Hull Resistance" *Ocean Eng.* Vol.110, Part B, December (2015), pp.2-10
- Campana E.F., Stern F., Diez M., "Hydrodynamic Ship Design Optimization Considering Uncertainty" *NAV 2015* (2015) pp.28-36
- Cao, H.J., Wan, D.C., "Benchmark computations of wave run-up on single cylinder and four cylinders by naoe-FOAM-SJTU solver", *Applied Ocean Research*, 2017, Vol. 65, pp. 327-337
- Cao, H.J., Wan, D.C., "Development of Multi-directional Nonlinear Numerical Wave Tank by naoe-FOAM-SJTU Solver", *International Journal of Ocean System Engineering*, 2014, Vol. 4, No. 1, pp. 52-59
- Ceccio, S.L. 2010 "Friction Drag Reduction of External Flows with Bubble and Gas Injection," *Annual Review of Fluid Mechanics*, vol. 42, pp. 183-203.
- Chang, H-C., Cheng, X., Liu, Z-Y., Feng, B-W., Zhan, C-S., "Sample Selection Method for Ship Resistance Performance Optimization Based on Approximated Model" *JSR*, Vol. 60, Number 1, March 2016, pp. 1-13 (13)
- Choi, H., Moin, P., and Kim, J., 1993, "Direct numerical simulation of turbulent flow over riblets," *Journal of Fluid Mechanics*, vol. 255, pp. 503-539.
- Choi, K.-S., 1989, "Near-wall structure of a turbulent boundary layer with riblets," *Journal of Fluid Mechanics*, vol. 208, pp. 417-458.
- Choi, K.-S., DeBisschop, J.-R., and Clayton, B. R., 1998, "Turbulent boundary-layer control by means of spanwise-wall oscillation", *AIAA Journal*, vol. 36, no. 7, pp. 1157-1163.
- Craft, T., Johnson, N., Launder, B. 2014 "Back to the future? A re-examination of the aerodynamics of Flettner-Thom rotors for maritime propulsion" *Flow, turbulence and combustion*. 92(1-2):413-27.
- Dadd, G.M., Hudson, D.A., Shenoi, R.A. 2011

- “Determination of kite forces using three-dimensional flight trajectories for ship propulsion” Renewable Energy 36,2667-2678.
- Dang J., 2012, “An exploratory study on the working principle of energy saving devices (ESDs)-PIV,CFD investigations and ESD design guidelines,” Proceedings of the 31<sup>st</sup> International Conference on Ocean, Offshore and Arctic Eng., OMAE2012-83053, Rio de Janeiro, Brazil.
- Dang J., Hao C., Rueda L., Willemsen H., “Integrated Design of Asymmetric Aftbody and Propeller for an Aframax Tanker to Maximize Energy Efficiency”, smp' 15 (2015) pp. 356-366.
- Diez M., Serani A., Stern F., Campana E.F., “Combined Geometry and Physics Based Method for Design-space Dimensionality Reduction in Hydrodynamic Shape Optimization” 31st SNH (2016).
- Dinham-Peren T., “Calculation of Optimum Trim Based on Bow and Stern Shape Functions” NAV 2015, (2015) pp.470-482.
- DNVGL, Maritime Energy Management Study 2015: Energy efficient operation-what really matters. 2015.
- Dong S-Z., Feng B-W., Shen T., Zhan C-S., Chang H-C., “CFD-based Hull Form Resistance and Flow Field Multi-objective Optimization Research” ISOPE 2014 Vol.4 pp.714-720.
- Druckenbrod M., Wang K., Greitsch L., Heinke H-J., Abdel-Maksoud M., “Development of hub caps fitted with PBCF”, smp' 15 (2015) pp.376-383.
- Du P., Wen J., Song D., Hu H., Ouahsine A., Zhang Z., “Maintenance of Air Layer and Drag Reduction on Superhydrophobic Surface” Ocean Eng. Vol.130, January (2017), pp.328-335.
- Dyne, G., 1995. The principles of propulsion optimization. Trans RINA, London, pp.189-201.
- Elbing, B. R., Winkel, E. S., Lay, K. A., Ceccio, S. L., Dowling, D. R. and Perlin, M., 2008, “Bubble-induced skin-friction drag reduction and the abrupt transition to air-layer drag reduction,” Journal of Fluid Mechanics, vol. 612, pp. 201-236.
- Elbing, B. R., Winkel, E. S., Solomon, M. J., and Ceccio, S. L., 2009, “Degradation of homogeneous polymer solutions in high shear turbulent pipe flow,” Experiments in Fluids, vol. 47, no. 6, pp. 1033-1044.
- Elbing, B.R., Makiharju, S., Wiggins, A., Perlin, M., Dowling, D.R., and Ceccio, S.L., 2013, “On the scaling of air layer drag reduction,” Journal of Fluid Mechanics, vol. 717, pp. 484-513.
- Elbing, B.R., Solomon, M.J., Perlin, M., Dowling, D.R. and Ceccio, S.L., 2011, “Flow-induced degradation of drag-reducing polymer solutions within a high-Reynolds number turbulent boundary layer,” Journal of Fluid Mechanics, vol. 670, pp. 337-364.
- Fagiano, L., Milanese, M., Razza, V., and Bonansone M. 2012 “High-Altitude Wind Energy for Sustainable Marine Transportation” IEEE TRANSACTIONS ON INTELLIGENT TRANSPORTATION SYSTEMS, VOL. 13, NO. 2
- Fahri Celik., “A numerical study for effectiveness of a wake equalizing duct”. Ocean Engineering, 2007, Vol.34, pp. 2138-2145.
- Flack, K.A., and Schultz, M.P., 2010, “Review of hydraulic roughness scales in the fully rough regime,” Journal of Fluids Engineering, vol. 132, 041203, 10 pages.

- Flack, K.A., and Schultz, M.P., 2014, "Roughness effects on wall-bounded turbulent flows," Physics of Fluids, vol. 26, 101305, 17 pages.
- Flack, K.A., Schultz, M.P. and Shapiro, T.A., 2005, "Experimental support for Townsend's Reynold number similarity hypothesis on rough walls," Physics of Fluids, vol. 17, 035102
- Flack, K.A., Schultz, M.P. and Shapiro, T.A., 2005, "Experimental support for Townsend's Reynold number similarity hypothesis on rough walls," Physics of Fluids, vol. 17, 035102
- Froude, R.E., 1883. A description of a method of investigation of screw-propeller efficiency, Trans INA, London, pp. 231-249.
- Fukagata, K., 2011, "Drag Reduction by Wavy Surfaces," Journal of Fluid Science and Technology, vol. 6, no. 1, pp. 2-13.
- Gad-el-Hak, M., 2002, "Compliant coatings for drag reduction," Progress in Aerospace Sciences, vol. 38, pp. 77-99.
- García-Mayoral, R. and Jiménez, J., 2011, "Drag reduction by riblets," Philosophical Transaction of Royal Society, Ser. A, vol. 369, pp. 1412-1427.
- Ginnis A-A.I., Duvigneau R., Politis C., Kostas K., Belibassakis K., Gerostathis T., Kaklis P. D., "a Multi-Objective Optimization Environment for Ship-Hull Design based on a BEM-Isogeometric Solver" MARINE 2013 (2013) pp.144-155.
- Go J.S., Yoon H.S., Jung J.H., "Effects of a Duct Before a Propeller on Propulsion Performance" Ocean Eng. Vol.136, May (2017), pp.54-66.
- Golovin K.B., James W. Gose J.W., Perlin M, Ceccio S.L., Tuteja A., "Bioinspired Surfaces for Turbulent Drag Reduction" Phil. Trans. R. Soc. A 2016 vol, 374 27 June (2016).
- Gose J.W., Golovin K., Tuteja A., Ceccio S.L., Perlin M., "Experimental Investigation of Turbulent Skin-Friction Drag Reduction Using Superhydrophobic Surfaces" 31st SNH (2016).
- Gose, J.W., Golovin, K., Boban, M. Mabry, J. M., Perlin, M. and Ceccio, S. L., 2016, "Characterization of superhydrophobic surfaces for drag reduction in turbulent flow," submitted to Journal of Fluid Mechanics.
- Guiard T., Leonard S., Mewis F., "The Becker Mewis Duct (®)-Challenges in Full-Scale Design and new Developments for Fast Ships" smp' 13 (2013) pp.519-527.
- Guin, M. M, Kato, H., Yamaguchi, H., Maeda, M., Miyanaga, M., 1996, "Reduction of skin friction by microbubbles and its relation with near-wall bubble concentration in a channel," Journal of Marine Science and Technology, vol. 1, pp. 241-254.
- Gyr, A. and Bewersdorff, HW, 2013, Drag reduction of turbulent flows by additives, Springer-Science, Dordrecht.
- Hämäläinen R., van Heerd J., "Energy Saving Possibilities in Twin or Triple Propeller Cruise Liners" smp' 13 (2013) pp.55-68.
- Hansen H., Hochkirch K., "Lean ECO-Assistant Production for Trim Optimisation", Compit' 13 (2013) pp.76-84.
- Hashim, A., Yaakob, O.B., Koh, K.K., Ismail, N. and Ahmed, Y.M., 2015, "Review of Micro-bubble Ship Resistance Reduction Methods and the Mechanisms that Affect the Skin Friction on Drag Reduction from 1999 to

- 2015,” *Jurnal Teknologi*, vol. 74 (5), UTM Press.
- Haslbeck, E. G. and Bohlander, G. S., 1992, “Microbial Biofilm Effects on Drag-Lab and Field,” U.S. Navy, Naval Surface Warfare Center Report, Carderock Division.
- He N.V., Mizutani K., Ikeda Y., “Reducing Air Resistance Acting on a Ship by using Interaction Effects between the Hull and Accommodation” *Ocean Eng.* Vol. 111, January (2016), pp.414-423.
- Hino T., Hirota M., “Flow Simulations of Japan Bulk Carrier Using Overset Grid Approach” *CWT2015 Vol.3*, pp.443-447.
- Hoang, C. L., Toda, Y., and Sanada, Y., 2009, “Full scale experiment for frictional resistance reduction using air lubrication method,” *Proc. 19<sup>th</sup> Int. Offshore Polar Eng. Conf.*, pp. 812-817.
- Hochkirch K., Heimann J., Bertram V., “Hull Optimization for Operational Profile-The Next Game Level” *MARINE 2013 (2013)* pp.81-88.
- Hochkirch K., Mallol B., “On the Importance of Full-Scale CFD Simulations for Ships”, *Compit' 13 (2013)* pp.85-95.
- Hori M., Jufuku N., Ito S., Hinatsu M., Toda Y., “Stern Flow Field Measurement around Japan Bulk Carrier Model with Rotating Propeller and Upstream Energy Saving Duct”, *Conference Proceedings of ISOPE 2016*, (2016), pp.883-889.
- Howett, B., Lu, R., Turan, O., & Day, A. H. 2015. “The use of wind assist technology on two contrasting route case studies” *Shipping in Changing Climates Conference (SCC)*, Glasgow, Scotland, UK, 24th-26th November 2015: p355.
- Hoyt, J.W., 1972, “Effects of additives on fluid friction,” *Journal of Basic Engineering*, vol. 94, no. 2, pp. 258-285.
- Hsieh Y-H., Lee S-K., Zhou A., “Design Evaluation of Energy-Saving Devices for Full Form Ship Propulsion” *compit' 13 (2013)* pp.437-449.
- Hu, H.Z., Su, Y.M., Sheng, H.L., et al., “Study on the energy saving effect of rudder thrust fins”, *Ship Science and Technology*, 2016, Vol. 38, No. 3, pp. 67-72.
- Hwang S., Kim M-S., Kim C., Lee Y-Y., Ahn H., Van S-H., Kim K., Jang Y-H., Kim M-H., Lee Y-S., “Experimental Study on Bow Hull-Form Modification for Reduction of Added Resistance in Waves for Mega-Size Container Ships” *PRADS 2016 (2016)*.
- Ichinose Y., Kume K., Tahara Y., “A Development and Analysis of the New Energy Saving Device “USTD”” *NuTTS 2016*, (2016) pp.49-54.
- Igeta M., Yuan H-B., “Development and Performance Estimates of a Ducted Tandem CRP” *smp' 13 (2013)* pp.161-167.
- Ikeda T., Kimura K., Taketani T., Ando S., Yamamoto K., “Advanced Propeller Design Optimization System Based on Open Source Codes and its Application” *PRADS 2016 (2016)*.
- Innovative Marine Solutions, 2016. Energy efficiency white paper. Ship Operations cooperative Program. Woodinville, Washington.
- International Maritime Organization (IMO). Buhaug, Ø., Corbett, J.J., Eyring, V., Endresen, Ø., Faber, J., Hanayama, S., Lee, D.S., Lee, D., Lindstad, H., Markowska, A.Z. and Mjelde, A., 2009. “Second IMO GHG Study” IMO, London, UK.

- Itoh, M., Tamano, S., Yokota, K., and Taniguchi, S., 2006, “Drag reduction in a turbulent boundary layer on a flexible sheet undergoing a spanwise traveling wave motion,” *Journal of Turbulence*, vol. 7, no. 27, DOI: 10.1080/14685240600647064.
- ITTC, 1978, “1978 ITTC Performance Prediction Method”. *ITTC Recommended Procedures and Guidelines*, section 7.5-02-03-01.4, Effective Date. 2014, Revision. 03.
- ITTC, 1999, “Final report of the specialist committee on unconventional propulsors”, *22<sup>nd</sup> International Towing Tank Conference*, Seoul Korea and Shanghai, China.
- Jagdish, B.N., Brandon, T. Z. X., Kwee, T-J., Dev, A. K., “Experimental Study of Air Layer Sustainability for Frictional Drag Reduction” *JSR*, Vol. 58, Number 1, March 2014, pp. 30-42(13).
- Jang J-H., Ahn S-M., Seo J-S., “Experimental Investigation of Air Layer on the Hull Bottom for Frictional Resistance Reduction of Ships”, *Proceedings of PRADS 2013*, (2013) pp.1044-1051.
- Jang, J., Choi, S. H., Ahn, S. M., Kim, B., Seo, J. S., 2014, “Experimental investigation of frictional resistance reduction with air layer on the hull bottom of a ship”, *International Journal of Naval Architecture and Ocean Engineering*, Vol. 6, pp 363-379.
- Jiang J-W., Cai H-P., Ma C., Ke C., “Multi-Objective Optimal Design of Ships Propeller Considering Fluid – Structure Interaction” *ISOPE 2016* (2016) Vol.4 pp.773-778.
- Jiménez, J., 2004, “Turbulent flows over rough walls,” *Annual Review of Fluid Mechanics*, vol. 36, pp.173-196.
- Jung Y-W., Kim Y., Park D-M., “Prediction of Ship Performance in Waves and Application to Hull-Form Design” *PRADS 2016* (2016).
- Kametani, Y. and Fukagata, K., 2012, “Direct numerical simulation of spatially developing turbulent boundary layer for skin friction drag reduction by wall surface-heating or cooling,” *Journal of Turbulence*, vol. 13, no. 34, DOI: 10.1080/14685248.2012.710750.
- Kametani, Y., Fukagata, K. Orlu, R. and Schlatter, P., 2015, “Effect of uniform blowing/suction in a turbulent boundary layer at moderate Reynolds number,” *International Journal of Heat and Fluid Flow*, vol. 55, 132-142.
- Kamiirisa H., Kawashima H., Makino M., “An Energy Saving Technique for Ships by Air Lubrication System”, *AMT' 15* (2015).
- Kano T., Namie S., “A Study on Estimation of GHG Emission for Speed Planning Operation Using Energy Efficiency Index and Time-Series Monitoring Data” *Compit' 14* (2014) pp.167-180.
- Kato, H., Miura, K., Yamaguchi, H., Miyahaga, M., 1998, “Experimental study on micro-bubble ejection method for frictional drag reduction,” *Journal of Marine Science and Technology*, vol. 3, pp. 122-129.
- Kawamura T., Ouchi K., Takeuchi S., “Model and Full Scale CFD Analysis of Propeller Boss Cap Fins (PBCF)” *smp' 13* (2013) pp. 486-493.
- Keirsbulck, L., Labraga, L., Mazouz, A. and Tournier, C., 2002, “Influence of surface roughness on anisotropy in a turbulent boundary layer flow,” *Experiments in Fluids*, vol. 33 (3), 497-499.
- Kim H-J., Choi J-E, Chun H-H., “Hull-Form Optimization Using Parametric Modification Functions and Particle Swarm Optimization” *JMST Vol. 21, Issue 1, March* (2016) pp.

- 129-144.
- Kim J-H., Kim Y-H., "Study on Optimal Routing Problem for Cruise Ship Design" IWSH 2013 (2013).
- Kim K.S., Kim M.C., Van S.H., Suh J.C., Lee J.T., 1994, "A Preswirl stator-Propeller system as a Reliable Energy-Saving Device," Proceedings of Propeller/Shafting'94 Symposium, Virginia Beach, pp. 9-1—9-16.
- Kim K-J., Leer-Andersen M., Orych M., "Hydrodynamic Optimization of Energy Saving Devices in Full Scale" 30th SNH (2014).
- Kim K-S., Roh M-I., Ham S-H., "Ship Route Planning Considering the Effects of Sea State and Fuel Consumption" PRADS 2016 (2016).
- Kim W., Jang Y., Kim M., "Performance Analysis for DSME Cap Fin in Model and Full Scale" PRADS 2016 (2016).
- Kim Y-S, Kim K-S., Jeong S-W., Jeong S-G., Van S-H., Kim Y-C., Kim J., "Design and Performance Evaluation of Superstructure Modification for Air Drag Reduction of a Container ship" ISOPE 2015 (2015) Vol.4, pp.894-901.
- Kim, M. C., Shin, Y.J., Lee, W.J., Lee, J.H., 2017, "Study on Extrapolation Method for Self-Propulsion Test with Pre-Swirl Device," 5<sup>th</sup> International Symposium on Marine Propellers (SMP '17), Espoo, Finland, June 2017.
- Kleinsorge E., Lindner H., Wagner J., Bronsart R., "Ship Hull Form Optimization using Scenario Methods" PRADS 2016 (2016).
- Kodama, Y., Kakugawa, A., Takahashi, T. and Kawashima, H., 2000, "Experimental study on microbubbles and their applicability to ships for skin friction reduction," International Journal of Heat Fluid Flow, vol. 21, pp. 582-588.
- Korkmaz K. B., Shen Z-R., Korpus R., "Numerical Simulations of Ship Self-Propulsion and Maneuvering Using Dynamic Overset Grids in Open-FOAM" CWT2015 Vol.3, pp. 221-226.
- Krogstad, P.A., Antonia, R.A. and Browne, L. W.B., 1992, "Comparison between rough- and smooth-wall turbulent boundary layers," Journal of Fluid Mechanics, vol. 245, 599-617.
- Kulik V.M., Boiko A.V., Chun H.H., Lee I., "Control for Flat Plate Skin-Friction Drag with Compliant Coatings (Predictions and Experiment)" EDRFCM 2015 (2015), pp. 113-114.
- Kunkel, G.J. and Marusic, I., 2006, "Study of near-wall-turbulent region of the high-Reynolds-number boundary layer using an atmospheric flow," Journal of Fluid Mechanics, vol. 548, 375-402.
- Kuroda M., Tsujimoto M., Sasaki N., Naito M., Omote M., Nojima N., kaga M., "Analysis on Onboard Measurement Data for the Validation of the Effect of the Energy Saving Device STEP", Conference Proceedings of PRADS 2013, pp.346-351.
- Lardeau, S. and Leschziner, M.A., 2013, "The streamwise drag-reduction response of a boundary layer subjected to a sudden imposition of transverse oscillatory wall motion," Physics of Fluids, vol. 27 (7), 075109.
- Larsson E., Simonsen M.H., Mao W-G., "DIRECT Optimization Algorithm in Weather Routing of Ships" ISOPE 2015 (2015) Vol. 4, pp.1207-1214.
- Lay, K. A., Yakushiji, R., Makiharju, S., Perlin, M., and Ceccio, S. L., 2010, "Partial cavity

- drag reduction at high Reynolds numbers,” Journal of Ship Research, vol. 54, no. 2, pp. 109-119.
- Lee H-D., Hong C-B., Kim H-T., Choi S-H., Han J-M., Kim B., Lee J-H., “Development and Application of Energy Saving Devices to Improve Resistance and Propulsion Performance” ISOPE 2015 (2015) Vol.4, pp.906-910.
- Lee H-J., Jo Y-M., Choi S-I., Kwon J-O., Ahn S-M., “Aerodynamic Analysis and Design Optimization of Wing-Sails”, Proceedings of PRADS 2013, (2013) , pp.959-970.
- Lee I., Chun H-H., “Experimental Procedures toward the Performance Assessment for Low Frictional Marine Paints” AMT' 13 (2013).
- Lee I., Park H., Chun H.H., “a Novel Drag-Reducing Coating Material: FDR-SPC (Frictional Drag Reduction Self-Polishing Copolymer)” EDRFCM 2015 (2015), pp.71-72.
- Lee S., Shin H-J., Yang J-H., Park, S-H., “Investigation on the Bow-Hull Forms of VLCC to Reduce Added Resistance in Different Loading Condition” PRADS 2016 (2016).
- Lee S-K., Yu K., Kuo-Cheng Tseng R., “Propeller Performance of a Containership Fitted with Energy-Saving Rudder Fin in a Seaway”, Proceedings of PRADS 2013, (2013) pp.226-234.
- Lee Y-M., Han M-R., Go S-C., “A Study on the Model test and Analysis Method for Energy saving Devices with Local Measurement System”, smp' 15 (2015) pp.252-258.
- Lee, J.T., Kim M.C., Van S.H., Kim K.S., Kim H.C., 1994, “Development of Preswirl Stator-Propeller System for a 300K VLCC,” Journal of the Society of Naval Architects of Korea, vol. 31, no. 1, pp.1-13.
- Lee, W. J., 2015, “Study on Full-Scale Performance Prediction for Pre-Swirl Device Model Test Results,” Ph. D. thesis, Pusan National University.
- Leonardi, S., Orlandi, P., Smalley, R. J. and Djenidi, L., 2003, “Direct numerical simulations of turbulent channel flow with transverse square bars on one wall,” Journal of Fluid Mechanics, vol. 491, 229-238.
- Lewkowciz, A.K. and Das, D.K., 1981, “Turbulent Boundary Layers on Roughness with and without a Pliable over Layer: A simulation of Marine Fouling,” Joint ASME/ASCE Bioengineering Fluid Mechanics and Applied Mechanics Conference, Boulder, CO, USA.
- Li, S-Z., Zhao, F., Ni, Q-J., “Bow and Stern Shape Integrated Optimization for a Full Ship by a Simulation-based Design Technique” JSR, Vol. 58, Number 2, June 2014, pp. 83-96(14).
- Li, W., Jessen, W., Roggenkamp, D. and Klaas, M., 2015, Turbulent drag reduction by spanwise traveling ribbed surface waves,” European Journal of Mech-B/Fluids, vol. 53, 101-112.
- Liaw, G.C., Zakin, J.L. and Patterson, G.K., 1971, “Effects of molecular characteristics of polymers on drag reduction,” AICHE Journal, vol. 17, no. 2, pp. 391-397.
- Lin, N.J., Miao, F., Huang, G.F., “Study on the optimal design of the pre-swirl stator”, Shipbuilding of China, 2014, Vol. 4, pp. 74-81.
- Lloyds Register Marine (2015) “Wind-powered shipping: A review of the commercial, regulatory and technical factors affecting uptake of wind-assisted propulsion” Technical Report. Published on line.
- Lloyds Register (2016) “2016 Workshop on

- Ship Scale Hydrodynamic Computer Simulation”, <http://www.lr.org/en/projects/findings-of-lrs-full-scale-numerical-modelling-workshop.aspx>.
- Luhar, M., Sharma, A.S. and McKeon, B.J., 2015, “A framework for studying the effect of compliant surfaces on wall turbulence,” Journal of Fluid Mechanics, vol. 768, 415-441.
- Lumley, J.L., 1969, “Drag reduction by additives,” Annual Review of Fluid Mechanics, vol. 1, pp. 367-387.
- Mäkiharju, S., Elbing, B.R., Wiggins, A.D., Schinasi, S., Vanden-Broeck, J.-M., Perlin, M., Dowling, D.R., Ceccio, S.L., 2013, “On the scaling of air entrainment from a ventilated partial cavity,” Journal of Fluid Mechanics, vol. 732, pp. 47-76.
- Mäkiharju, S., Perlin, M., and Ceccio, S.L., 2012, “On the energy economics of air lubrication drag reduction,” International Journal of Naval Architecture and Ocean Engineering, vol. 4, pp. 412-422.
- Mamori, H. and Fukagata, K., 2011, “Drag reduction by streamwise traveling wave-like Lorenz Force in channel flow,” Journal of Physics, Conference Series 318, 022030.
- Maria Viola I., Sacher M., Xu J., Wang F., “A Numerical Method for the Design of Ships with Wind-assisted Propulsion” Ocean Eng. Vol.105, September (2015), pp.33-42.
- MariaViola, I., Sacher, M., Xu, J., Wang, F. 2015 “A numerical method for the design of ships with wind-assisted propulsion” Ocean Engineering105: 33-42.
- Marrion, A.R., Ed., 2004, The Chemistry and Physics of Coatings, Roy. Soc. Chemistry, Cambridge, U.K.
- Matveev, K. I., 2003, “Technical note on the limiting parameters of artificial cavitation,” Ocean Engineering, vol. 30, pp. 1179-1190.
- McComb, W., 1990, The physics of fluid turbulence. Oxford University Press, Oxford, UK.
- Meng, Q.J., Wan, D.C., “URANS Simulations of Complex Flows Around a Ship Entering a Lock with Different Speeds”, International Journal of Offshore and Polar Engineering, 2016, Vol. 26, No. 2, pp. 161-168.
- Merkle, C. L. and Deutsch, S., 1992, “Drag reduction in liquid boundary layers by gas injection”, Progress in Astronautics and Aeronautics, vol. 123, pp. 351-412.
- Mewis F. and Guiard T., 2011, “Mewis duct-new developments, solutions and conclusions,” Proceedings of the 2<sup>nd</sup> International Symposium on Marine Propulsors, Hamburg, Germany.
- Milne, A., 2004, “Economics and the Environment: The Role of Coatings,” Chapter 1, The Chemistry and Physics of Coatings, Marrion, A.R., Ed., 1-7.
- Min, T., Kang, S.M., Speyer, J.L., and Kim, J., 2006, “Sustained sub-laminar drag in a fully developed channel flow,” Journal of Fluid Mechanics, vol. 558, pp. 309-318.
- Minchev A., Schmidt M., Schnack S., “Contemporary Bulk Carrier Design to Meet IMO EEDI Requirements” smp' 13 (2013) pp. 283-291.
- Mizokami, S., Kawakita, C., Kodan, Y., Takano, S., Higasa, S., and Shigenaga, R., 2010, “Experimental Study of Air Lubrication Method and Verification of Effects on Actual Hull by Means of Sea Trial,” Mitsubishi Heavy Industries Technical Review, vol. 47, no. 3, pp. 41-47.
- Molland, A.F., Turnock, S.R. and Hudson, D.

- A., "Ship resistance and propulsion: practical estimation of propulsive power" Cambridge university press. (2011).
- Molland, A.F., Turnock, S.R., Hudson, D.A. and Utama, I.K.A.P., "Reducing ship emissions: a review of potential practical improvements in the propulsive efficiency of future ships" Transactions of Royal Institution of Naval Architects Part A, 156, (2014) pp.175-188.
- Moriguchi, Y., and Kato, H., 2002, "Influence of microbubble diameter and distribution on frictional resistance reduction," Journal of Marine Science and Technology, 7, pp. 79-85.
- Muhdar Tasrief M., Kashiwagi M., "Optimization of Sectional Area Curve of a Ship" IWSH 2013 (2013).
- Murai, Y., 2014, "Frictional drag reduction by bubble injection", Experiments in Fluids, vol. 55, pp. 1-28.
- Murai, Y., Fukuda, H., Oishi, Y., Kodama, Y., Yamamoto, F., 2007, "Skin friction reduction by large air bubbles in a horizontal channel flow," International Journal of Multiphase Flow, vol. 33, pp. 147-163.
- Naaijen, P. & Koster V. 2007 "Performance of auxiliary wind propulsion for merchant ships using a kite" 2nd International Conference on Marine Research and Transportation. 45-53.
- Nagel R., "A Holistic Approach for Energy Flow Simulations in Early Design" compit 14, (2014) pp.41-48.
- Nieuwstadt, F. T. M. and Den Toonder, J., 2001, "Drag reduction by additives: a review," In: Soldati, A and Monti, R. (eds) Turbulence structure and motion. Springer, New York, pp. 269-316.
- Nikuradse, J., 1933, "Laws of flow in rough pipes," NACA Technical Memorandum 1292.
- Nishikawa T., "Application of Fully Resolved Large Eddy Simulation to Japan Bulk Carrier with an Energy Saving Device" CWT2015 Vol.3, pp.407-412.
- Nojiri, T., Ishii, N., Kai, H., "Energy Saving Technology of PBCF (Propeller Boss Cap Fins) and its Evolution" Journal of the Marine Engineering Society in Japan, 2011, Vol. 46, No. 3, pp. 350-358.
- OCIMF (Oil Companies International Marine Forum), GHG Emission-Mitigating Measures for Oil Tankers. Part A: Review of reduction potential (2011).
- Oh S., Choi S., Kim T., Lee D., Kim B., "The Study on the Tank Test Techniques for the Added Resistance in Waves", KTTTC Annual Spring Meeting 2017.
- Oil Companies International Marine Forum (OCIMF) 2011. GHG Emission-Mitigating Measures for Oil tankers: Part A; Review of reduction potential.
- Okada Y., Kawasaki M., Katayama K., Okazaki A., Fukuda K., Okazaki M., "The development of "Ultimate Rudder" for EEDI" MA-RINE 2015 (2015) pp.605-612.
- Okazaki M., Okada Y., Katayama K., Kajihama T., "Propeller Particulars and Scale Effect Analysis of ECO-Cap by CFD", NuTTS 2015 (2015).
- Olsen G.L., "e-Navigation Starts with e-VoyagePlanning", Compit' 13 (2013) pp.135-142.
- Ouchi K., Uzawa K., Kanai A., Katori M., "Wind Challenger" the Next Generation Hybrid Sailing Vessel" smp' 13 (2013) pp.

- 562-567.
- Ouchi K., Zhu T., Hirata J. Tanaka Y. Akira Taniguchi A., Kawagoe Y., Hisajima T., Takashina J., Matsubara N., Suzuki K., "A Research On Decreasing Wind Resistance Of Large Containership" RINA EES 2015 (2015).
- Paik B.G., Kim K-Y., Kim J-H., Cho S-R., Ahn J-W., Cho S-R., Kim K-R., . Chung Y-U., "Flat Plate Model Test for the Evaluation of Skin Friction in the Cavitation Tunnel" AMT' 13 (2013).
- Paik B-G., Kim K-Y., Cho S-R., Ahn J-W., Cho S-R., "Investigation on Drag Performance of Anti-fouling Painted Flat Plates in a Cavitation Tunnel" Ocean Eng. Vol.101, June (2015), pp.264-274.
- Pang M.J., Wei J.J., B. Yu B., "Numerical Study on Modulation of Micro Bubbles on Turbulence Frictional Drag in a Horizontal Channel" Ocean Eng. Vol.81, May (2014), pp. 58-68.
- Pao, X., Yang, Y.S., "Simulation on Super-cavitation Characteristics of Underwater Vehicle", Equipment Manufacturing Technology, 2015, Vol.4, pp. 243-244.
- Park H-G., Choi J-K., Kim H-T., "An Estimation Method of Full Scale Performance for Pulling Type Podded Propellers" smp' 13 (2013) pp.78-86.
- Park J-Y., Lee, S., Park, D., "Systematic Propeller Optimization considering hull interaction based on CFD" PRADS 2016 (2016).
- Park S., Oh G., Rhee S-H., Koo B-Y., Lee H., "Full Scale Wake Prediction of an Energy Saving Device by using Computational Fluid Dynamics" Ocean Eng. Vol. 101, June (2015), pp.254-263.
- Park S-H., Chun H-H., Lee I., "Optimization of Drag Reduction Effect of Air Lubrication for a Tanker Model based on Air Layer Observation" 31st SNH (2016).
- Park S-H., Oh G-H., "Numerical Multi-scale Analysis of Turbulent Flow Around Low-speed Ship with Energy Saving Pre-swirl Stator", Conference Proceedings of ISOPE 2014 (2014) pp.961-966.
- Park, H., An, N. H., Hutchins, N., Choi, K.-S., Chun, H. H., Lee, I., 2011, "Experimental investigation on the drag reducing efficiency of the outer-layer vertical blades," Journal of Marine Science and Technology, vol. 16, pp. 390-401.
- Patterson, R. W. and Abernathy, F. H., 1970, "Turbulent flow drag reduction and degradation with dilute polymer solutions", Journal of Fluid Mechanics, vol. 43, no. 4, pp. 689-710.
- Pearson, D. R. "The use of flettner rotors in efficient ship design." Proceedings of the Influence of EEDI on Ship Design Conference. 2014. 24-25 September, RINA, London, UK.
- Peet, Y. and Sagaut, P., 2009, "Theoretical prediction of turbulent skin friction on geometrically complex surfaces," Physics of Fluids, vol. 21, 105105 (21 pages).
- Pereira, A.S. and Soares, E.J., 2012, "Polymer degradation of dilute solutions in turbulent drag reducing flows in a cylindrical double gap rheometer device," Journal of Non-Newtonian Fluid Mechanics, vol. 179-180, 9-22.
- Perlin, M. and Ceccio, S.L., 2015, Mitigation of Hydrodynamic Resistance, World Sci. Publishing, Singapore.
- Perlin, M., Dowling, D.R. and Ceccio, S.L., 2016, "Freeman Scholar Review: Passive

- and Active Skin-Friction Drag Reduction in Turbulent Boundary Layers,” Journal Fluids Engr., vol. 138 (9), 091104,16 pp.
- Perry, A.E., Schofield, W.H. and Joubert, P.N., 1969, “Rough wall turbulent boundary layers,” Journal of Fluid Mechanics vol. 37 (2), 383-413.
- Picologlou, B.F., Charcklis, W.G. and Zelter, N., 1980, “Biofilm Growth and Hydraulic Performance,” Journal of the Hydraulics Division, ASCE, vol. 106 (5), 733-746.
- Rao Z-O., Li W., Yang C-J., “Simulation of Unsteady Interaction Forces on a Ducted Propeller with Pre-swirl Stators” smp' 13 (2013) pp.149-155.
- Report of 22th ITTC Specialist Committee on Unconventional Propulsors.
- Report of 27th ITTC Propulsion Committee.
- Report of 27th ITTC Resistance Committee.
- Rickard E Bensow, “Large Eddy Simulation of a Cavitating Propeller Operating in Behind Conditions with and without Pre-Swirl Stators” 4th International Symposium on Marine Propulsors smp' 15 (2015).
- Riley, J.J., Gad-el-Hak, M., and Metcalfe, R. W., 1988, “Compliant coatings,” Annual Review of Fluid Mechanics, vol. 20, pp. 393-420.
- Rothstein, J. P., 2010, “Slip on Superhydrophobic Surfaces,” Annual Review of Fluid Mechanics, vol. 42, pp. 89-109.
- Rueda L., Dang J., “Integrated Design of Asymmetric Aftbody and Propeller to Maximize Energy Efficiency”, RINA EES 2015 (2015).
- Ryu T., Kanemaru T., Kataoka S., Arihama K., Yoshitake A., Arakawa D., “Optimization of Energy Saving Device Combined with a Propeller Using Real-coded Genetic algorithm”, Proceedings of PRADS 2013, (2013) pp.218-225.
- Sakamoto N, Kawanami Y., Hinatsu M. , and Uto S., “Viscous CFD Analysis of Stern Duct Installed on Panamax Bulk Carrier in Model and Full Scale”, Proceedings of 13th International Conference on Computer and IT Application in the Maritime Industries, compit' 14, (2014) pp.72-82.
- Sakurada A., Tsujimoto M., Kuroda M., “Development of COVE Bow-Energy Saving Bow Shape in Actual Seas” PRADS 2016 (2016).
- Salonen S., Heikkinen A., “Robust Characterization of Ship Power Plant Fuel Efficiency”, compit' 13 (2013), pp.293-299.
- Sánchez-Caja A., Pérez-Sobrino M., Quereda R., Nijland M., Veikonheimo T., González-Adalid J., Saisto I., Auriarte A., “Combination of Pod, CLT and CRP Propulsion for Improving Ship Efficiency: the TRIPOD Project” smp' 13 (2013) pp.347-357.
- Sanders, W. C., Winkel, E. S., Dowling, D. R., Perlin, M. and Ceccio, S. L., 2006, “Bubble friction drag reduction in a high-Reynolds-number flat-plate turbulent boundary layer,” Journal of Fluid Mechanics, vol. 552, pp. 353-380.
- Saravi, S.S. and Cheng, K., 2013, “A review of drag reduction by riblets and micro-textures in the turbulent boundary layers,” European Scientific Journal, vol. 9 (33), 62-81.
- Sasaki N., Adler M., Kuribayashi S., “Advantages of Twin Rudder System With Asymmetric Wing Section Aside A Propeller” JMST Vol.21 Issue 2, June (2016) pp.297-308.

- Scholcz T.P., Gornicz T., Veldhuis C., “Multi-objective hull-form optimization using Kriging on noisy computer experiments” MARINE 2015 (2015) pp.1064-1077.
- Schrader L.U., “Drag Reduction for Ships Inspired by Dolphins”, NuTTS 2015, (2015).
- Schuiling B., “The Design and Numerical Demonstration of a New Energy Saving Device”, NuTTS 2013 (2013).
- Schultz, M. P. and Flack, K. A., 2007, “The rough-wall turbulent boundary layer from the hydraulically smooth to the fully rough regime,” Journal of Fluid Mechanics, vol. 580, 381-405.
- Schultz, M.P. and Swain, G.W., 1999, Journal of Fluids Engineering, vol. 121 (1), 44-51.
- Schultz, M.P., 1998, “The Effect of Biofilms on Turbulent Boundary Layer Structure, Ph. D. Thesis, Florida Institute of Technology.
- Schultz, M.P., 2004. “Frictional resistance of antifouling coating systems,” Journal of Fluids Engineering, vol. 126, pp.1039-1047.
- Sellin, R. H. J., Hoyt, J. W., Pollert, J., and Scrivener, O., 1982, “The effect of drag reducing additives on fluid flows and their industrial applications: Part II. Basic applications and future proposals,” J. Hyd. Res., vol. 20, no. 3, pp. 235-292.
- Seo J., García-Mayoral R., Mani A., “Turbulent Flows Over Superhydrophobic Surfaces: Gas-Liquid Interface Dynamics” 30th SNH (2014).
- Seo, J-H., Lee S-J., Han, B-W., Rhee, S-H., “Influence of Design Parameter Variations for Propeller-Boss-Cap-Fins on Hub Vortex Reduction” JSR Vo. 60, Number 4, Dec. 2016, pp. 203-218(16).
- Seo. J. and Mani, A., 2016, “On the scaling of the slip velocity in turbulent flows over superhydrophobic surfaces,” Physics of Fluids, vol. 28, 025-110.
- Shamsi R., Ghassemi H., Molyneux D., Liu P., “Numerical Hydrodynamic Evaluation of Propeller (With Hub Taper) and Podded Drive in Azimuthing Conditions” Ocean Eng. Vol.76, January (2014), pp. 121-135.
- Shen T., Feng B-W., Liu Z-Y., “A Hull Form Modification Method Based on Radial Basis Function and Its Application in Inverse Hull Optimization” ISOPE 2014 (2014) Vol.4pp. 726-730.
- Shen, Z. R., Wan, D. C., “An Irregular Wave Generating Approach Based on naoe-FOAM-SJTU Solver”, China Ocean Engineering, 2016, Vol. 30, No. 2, pp. 177-192.
- Shen, Z.R., Wan, D.C., Carrica, P., “Dynamic overset grids in OpenFOAM with application to KCS self-propulsion and maneuvering”, Ocean Engineering, 2015, Vol. 108, pp. 287-306.
- Shen, Z.R., Wan. D.C., “The Manual of CFD solver for ship and ocean engineering flows: naoe-FOAM-SJTU”, Shanghai Jiao Tong University, 2014, No.2012SR118110.
- Shen, Z.R., Ye, H., Wan, D.C., “URANS Simulations of Ship Motion Responses in Long-crest Irregular Waves”, Journal of Hydrodynamics, 2014, Vol. 26, No.3, pp. 436-446.
- Sheng, H.L, Cai, H.P, Su, Y.M., “Theoretical prediction method of energy saving effect of energy saving device in front of propeller” Journal of Shanghai Jiao Tong University, 2010, Vol. 44, No. 10, pp. 1418-1422.
- Shin H.J., Lee J.S., Lee K.H., Han M.R, Hur E.B., Shin S.C., 2013, “Numerical and experimental investigation of conventional and unconventional preswirl duct for VLCC,” International



- Journal of Naval Architecture and Ocean Engineering, vol. 5, no. 2, pp. 414-430.
- Shon, Y-E., Han S-H., Park, K-S., Son, S-H., “Design of Flow Adapted Rudder through the Linkage among CAD, CFD and Optimization Tool” PRADS 2016 (2016).
- Silberschmidt N., “Air Lubrication: From Concept, to Sea Trials, to Commercialisation” RINA EES 2015.
- Simpson, R. L., Moffat, R. J., and Kays W. M., 1969, “The turbulent boundary layer on a porous plate: experimental skin friction with variable injection and suction,” International Journal of Heat Mass Transfer, vol. 12, pp. 771-789.
- Skote, M., 2014, “Scaling of the velocity profile in strongly drag reduced turbulent flows over an oscillating wall,” International Journal of Heat and Fluid Flow, vol. 50, 352-358.
- Skudarnov, P.V., Lin, C.X., “Drag reduction by gas injection into turbulent boundary layer: Density ratio effect”, International Journal of Heat & Fluid Flow, 2006, Vol. 27, No. 3, pp. 436-444.
- Slyozkin A., Atlar M., Sampson R., Seo K-C., “An Experimental Investigation into the Hydrodynamic Drag Reduction of a Flat Plate Using Air-Fed Cavities” Ocean Eng. Vol. 76, January (2014), pp. 105-120.
- SOCP (Ship Operations Cooperative Program) and Glosten. 2016 “Energy Efficiency Report”, Job 15099.01, Rev A.
- Song B-W., Wang Y-J., Tian W-L., “Open Water Performance Comparison between Hub-type and Hubless Rim Driven Thrusters based on CFD Method” Ocean Eng. Vol. 103, July (2015), pp.55-63.
- Song H.J., Kim M.C., Lee W.J., Kim J.H., 2015, “Development of the New Energy Saving Device for the Reduction of Fuel of 176k Bulk Carrier,” Journal of the Society of Naval Architects of Korea, vol. 52, no. 6, pp. 419-427.
- Spalart, P.R., Strelets, M., and Travin, A., 2006, “Direct numerical simulation of large-eddy-break-up devices in a boundary layer,” International Journal of Heat and Fluid Flow, vol. 27, pp. 902-910.
- Srinivasan S., Kleingartner J.A., Gilbert J.B., Cohen R.E., Milne A.J.B., McKinley G.H., “Sustainable Drag Reduction in Turbulent Taylor-Couette Flows by Depositing Sprayable Superhydrophobic Surfaces” Phys. Rev. Lett. Vol 114, (2015) 6 January (2015).
- Streckwall H., Xing-Kaeding Y., Gatchell S., “Design of combined propeller/stator propulsion systems with special attention to scale effects” MARINE 2015 (2015) pp.568-578.
- Sun, J-L., Tu, H-W., Chen, Y-N., Xie, D., Zhou, J-J., “A Study on Trim Optimization for a Container Ship Based on Effects due to Resistance” JSR, Vol. 60, Number 1, March 2016, pp. 30-47(18).
- Sun, T., Wan, D.C., “Study of energy saving effect for product”, Chinese Journal of Hydrodynamics, 2016, Vol. 31, No. 6, pp. 651-658.
- Tahara Y., Ichinose Y., Kaneko A., Kasahara Y., “Application of Simulation Based Design for ESD Installed Commercial Ships” 31st SNH (2016).
- Tamano S., Kurisaki H., Ikarashi H., Morinishi Y., “Turbulent Drag Reduction Due to Electrostatic Flocking Surface with Grooves” EDRFCM 2015 (2015), pp.45-46.
- Tamano, S. and Itoh, M., 2012, “Drag reduction in turbulent boundary layers by spanwise traveling waves with wall deforma-

- tion,” Journal of Turbulence, vol. 13, DOI:
- Tomiyaama, N. and Fukagata, K., 2013, “Direct numerical simulation of drag reduction in a turbulent channel flow using spanwise traveling wave-like wall deformation,” Physics of Fluids, 25, 105115.
- Townsend, A.A., 1976, The Structure of Turbulent Shear Flow, Cambridge University Press, Cambridge, UK.
- Traut, M., Gilbert, P., Walsh, C., Bows, A., Filippone, A., Stansby, P. and Wood, R., 2014. “Propulsive power contribution of a kite and a Flettner rotor on selected shipping routes” Applied Energy, 113, pp.362-372.
- van der Ploeg A., “RANS-based optimization of the aft part of ships including free surface effects” MARINE 2015 (2015) pp.242-253.
- van der Ploeg A., van der Bles G., van Zelder- en J., “Optimization of a ship with a large diameter propeller”, NuTTS 2016, (2016) pp.102-107.
- van Terwisga T., “On the Working Principles of Energy Saving Devices” smp' 13 (2013) pp.510-517.
- Vanapalli, S.A., Ceccio, S.L., and Solomon, M. J., 2006, “Universal scaling for polymer chain scission in turbulence,” Proc. Natl. Acad. Sci., vol. 103, no. 45, pp. 16660-16665.
- Virk, P.S., 1975, “Drag reduction fundamentals,” AICHE Journal, vol. 21, no. 4, pp. 625-656.
- Volino, R.J., Schultz, M.P., and Flack, K. A., 2011, “Turbulence structure in boundary layers over periodic two-ann three-dimensional roughness,” Journal of Fluid Mechanics, vol. 676, 172-190.
- Walker J.M., Schultz M.P., Flack K.A., Steppe C.N., “Skin-Friction Drag Measurements on Ship Hull Coating Systems” 30th SNH (2014).
- Walsh, M. J., 1983, “Riblets as a Viscous Drag Reduction Technique,” AIAA Journal, vol. 21, no. 4, pp. 485-486.
- Wang, J.H., Wan, D.C., “Numerical simulation of pure yaw motion using dynamic overset grid technology”, Chinese Journal of Hydrodynamics, 2016, Vol. 31, No. 5, pp. 567-574.
- Wang, J.H., Wan, D.C., “Numerical simulation of pure yaw motion using dynamic overset grid technology”, Chinese Journal of Hydrodynamics, 2016, Vol. 31, No. 5, pp. 567-574.
- Wang, Z.Z, Xiong, Y., et al., “Numerical investigation of the scale effect of hydrodynamic performance of the hybrid CRP pod propulsion system”, Applied Ocean Research, 2016, Vol. 54, pp.26-38.
- West, N., Sammut, K. and Tang, Y., 2016, “Material selection and manufacturing of riblets for drag reduction: An updated review,” Proc. Institution Mech Engineers, Part L: Journal of Materials: Design and Applications.
- White, C.M. and Mungal, M.G., 2008, “Mechanics and prediction of turbulent drag reduction with polymer additives,” Annual Review of Fluid Mechanics, vol. 40, pp. 235-256.
- Winkel, E. S., Oweis, G. F., Vanapalli, S. A., Dowling, D.R., Perlin, M., Solomon, M.J., Ceccio, S.L., 2009, “High Reynolds number turbulent boundary layer friction drag reduction from wall-injected polymer solutions,” Journal of Fluid Mechanics, vol. 621, pp. 259-288.
- Wu, J.W., Liu, S.Y., Wan, D.C., “Multi-Objec-

- tive Hydrodynamic Optimization of Ship Hull Base on Approximation Model” ISOPE 2016, Vol.4, pp.814-820.
- Wu, J.W., Yin, C.H., Wan, D.C., “Numerical prediction of the propeller open-water performance based on three numerical methods”. *Chinese Journal of Hydrodynamics*, 2016, Vol. 31, No. 2, pp. 177-187.
- Xu, Q.X., “The Micro-bubble Drag resistance Technology”, Master thesis, Wuhan University of Technology, 2013.
- Yakeno, A. Hasegawa, Y. and Kasagi, N., 2014, “Modification of quasi-streamwise vertical structure in a drag-reduced turbulent channel flow with spanwise wall oscillation,” *Physics of Fluids*, vol.26 (8), 085109.
- Yan X-K., Gatchell S., Streckwall H., “Towards Practical Design Optimization of Pre-Swirl Device and its Life Cycle Assessment”, smp' 15 (2015) pp.318-329.
- Yang, J. W., Park, H., Chun, H. H., Ceccio, S. L., Perlin, M. and Lee, I., “Development and performance at high Reynolds number of a skin-friction reducing marine paint using polymer additives,” *Ocean Engineering*, Vol. 84, (2014), pp 183-193.
- Ye, H. X., Wan, D. C., “Benchmark computations for flows around a stationary cylinder with high Reynolds numbers by RANS-overset grid approach”, *Applied Ocean Research*, 2017, Vol. 65, pp. 315-326.
- Yeginbayeva I., Atlar M., Turkmen S., Kidd B., Finnie A. A., “Investigating the Impact of Surface Condition on the Frictional Resistance of Fouling Control Coating Technologies” 31st SNH (2016).
- Yin, C.H., Wu, J.W., Wan, D.C., “A Numerical Study for Self-propelled JBC with and without Energy Saving Device”, *Proceedings of Tokyo 2015 Workshop on CFD in Ship Hydrodynamics*, Vol. III, Dec. 2-4, 2015, NMRI, Tokyo, Japan, pp. 395-400.
- Yoon M., Ahn J-S., Hwang J-Y., Sunga H-J., “Contribution of Velocity-Vorticity Correlations to the Frictional Drag in Wall-Bounded Turbulent Flows” *Physics of Fluids*, Vol 28, Aug. (2016).
- Yuhai, Kong W-P, Cai R-Q, Wang J-B, Zhang Y-F., “Numerical Study of Energy-saving Mechanism of Duct on a VLCC with Real-geometry Propeller” smp'13 (2013) pp.528-534.
- Zhang J-X., Yao Z-H., Hao P-F., “Drag Reductions and the Air-Water Interface Stability of Superhydrophobic Surfaces in Rectangular Channel Flow” *Phys. Rev. E* 94 (2016) 22 November (2016).
- Zhang, T., Yang, C. J., Song, B-W., et al., “CFD simulation of unsteady performance of CRPs”, *Journal of Ship Mechanics*, 2011, Vol. 15, No .6, pp.605-615.
- Zou G, Kinnunen A., Tervo K., Orivuori J., Vänskä K., Tammi K., “Evaluate Ship Energy Saving Scenarios Using Multi-Domain Energy Flow Simulation” *Compit'14* (2014) pp.408-417.
- Zverkhovskiy O., Delfos R., Westerweel J., van Terwisga T., “Flat Plate Drag Reduction By An Air Cavity” *AMT' 13* (2013).
- Zverkhovskiy O., van Terwisga T., Gunging M., Westerweel J., Delfos R., “Experimental Study on Drag Reduction by Air Cavities on a Ship Model” 30th SNH (2014).
- Zverkhovskiy, O., 2014, “Ship drag reduction by air cavities,” Ph.D. Thesis, Delft University of Technology.